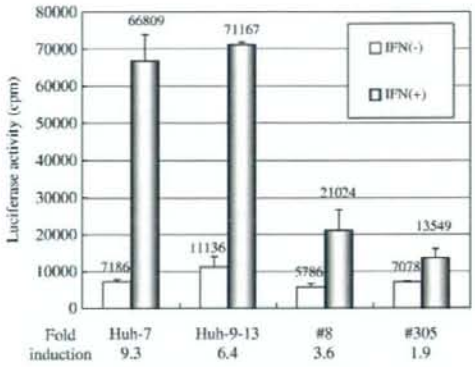

Fig. 4. Transactivation of ISRE in IFNα-resistant replicon cell lines (#8 and #305), original replicon (Huh-9-13), and parental Huh-7 cells by reporter gene (pISRE/Luc) analysis. The cells were stimulated with 1000 IU/mL of IFNα for 24 h after transfection of reporter plasmid DNA. White bars show control (no addition of IFNα) luciferase activity, and black bars show the activity under IFNα stimulation. Values of luciferase activity by IFNα stimulation relative to those of untreated cells are shown below the panel as 'fold induction'.

in a dsRNA-dependent manner, and transduce IFN production signals through the activation of nuclear factor κB (NFκB) and interferon regulatory factor 3 (IRF-3).

Despite bearing an HCV-1b genotype-derived replicon with mutations in ISDR, the replicon cells do not show resistances to IFN (Frese et al., 2002; Guo et al., 2001, 2004). Concerning this point, some reports regarding IFN-resistance acquisition and analysis of this property in the replicon cells (Namba et al., 2004; Sumpter et al., 2004; Zhu et al., 2005) showed involvement of various factors such as viral and/or host gene alterations participating in IFNα-resistance in replicon cells.

Here, we isolated IFNα-resistant clones of the HCV subgenome with accumulated mutations, especially in NS3 and NS5A regions. We observed impairment of phosphorylation of Stat-1 in cells bearing the IFNα-resistant HCV replicon. Our findings suggest that NS5A contributes to the acquisition of IFNα-resistant phenotype in HCV replicon cells.

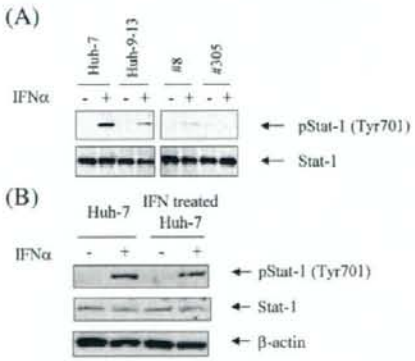

Fig. 5. (A) Change in phosphorylation of Stat-1 in IFNα-resistant replicon cell lines (#8 and #305), original replicon (Huh-9-13) and parental Huh-7 cell. Phosphorylation of Stat-1 was analyzed by western blot analysis using anti-phospho-Stat-1 (Tyr701) antibody. The cells were cultured in medium with or without 500 IU/mL of IFNα for 30 min. Upper panel represents a phospho-Stat-1 (Tyr701) and lower panel shows a Stat-1. Western blot analysis was performed as described in Materials and methods. (B) Change in phosphorylation of Stat-1 in Huh-7 cells maintained in the presence or absence of IFNα (10 IU/mL) for 4 weeks. Upper panel represents a phospho-Stat-1 (Tyr701), middle panel shows a Stat-1 and lower panel shows a β-actin. Phosphorylation of Stat-1 in these cells was examined as described above.

Results

Establishment of IFNα-resistant replicon cell lines

HCV replicon cells were cultured for approximately 1 month in the presence of 10 IU/mL IFNα. HCV RNA titer decreased during the culture; however, the appearance of cells less sensitive to IFNα during prolonged culture was observed by quantitative RT-PCR. The resistant cells were then cloned by limiting dilution. Three clones (Fig. 1: #6, #8, and #9) were obtained, and mixed pools of these resistant cells were further selected in the presence of 30 IU/mL IFNα for another 4 weeks. After confirming decreased sensitivity to IFNα at this dose, the clone

(A)

	Cell	IFN selection	EC50 (IU/mL)	Fold Reduction
Total RNA transfection	Huh-9-13/Huh-7	(-)	0.7	1.0
	#305/Huh-7	(-)	4.1	5.9
original	Huh-9-13	(-)	0.6	1.2

(B)

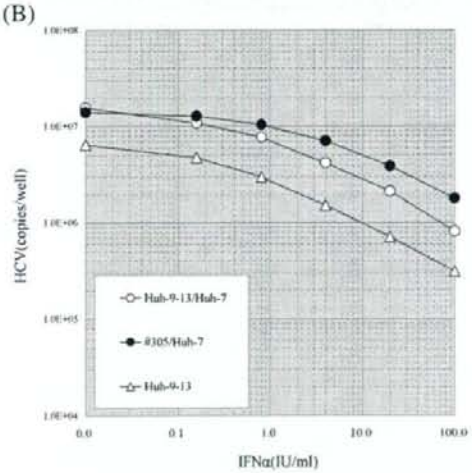

Fig. 6. Reactivity for IFNα in the Huh-7 cells, #305/Huh-7, transfected with total RNA of #305 replicon cells and in the Huh-7 cells, Huh-9-13/Huh-7, transfected with total RNA of original replicon cells (Huh-9-13). These transfected cells were selected with G418 in the absence of IFNα. The amount of HCV RNA was analyzed by quantitative RT-PCR, as described in Fig. 2. (A) EC_{50} value (IU/mL) of IFNα in Huh-9-13/Huh-7 and #305/Huh-7. (B) Change in copy number of HCV RNA in Huh-9-13/Huh-7 and #305/Huh-7 by IFNα treatment. These experiments were performed in triplicate and mean values are shown.

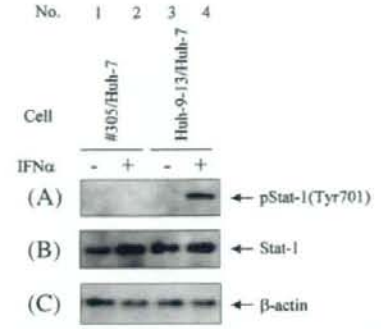

Fig. 7. Phosphorylation of Stat-1 in #305/Huh-7 and Huh-9-13/Huh-7 described in Fig. 6. The experiment was performed as described in Fig. 5. Each panel shows (A) phospho-Stat-1 (Tyr701), (B) Stat-1, and (C) β-actin. (Lanes 1 and 2) Huh-7 cells transfected with IFNα-resistant replicon (#305) total RNA (#305/Huh-7). (Lanes 3 and 4) Huh-7 cells transfected with original replicon (Huh-9-13) total RNA (Huh-9-13/Huh-7).

(Fig. 1; #305) showing highest resistance to IFNα was obtained. Sensitivities of these clones to IFNα are shown in Fig. 2. The basal HCV RNA levels in these cells (#6, #8, #9, and #305) were almost equal to that in the original replicon cells (Huh-9-13). The EC_{50} value of IFNα for the original replicon (Huh-9-13) was 0.7 IU/mL, compared to 6.9 IU/mL, 6.7 IU/mL, 10.2 IU/mL, and 99.2 IU/mL for resistant clones #6, #8, #9, and #305, respectively. These results demonstrate that sensitivity to IFNα based on EC_{50} value decreased 9 to 135-fold in the IFNα-resistant clones.

Characterization of IFNα-resistant replicon cell lines

First, expression of HCV NS proteins (NS3, NS5A, and NS5B) in IFNα-resistant replicon cell lines (#6, #8, #9, and #305) was analyzed by western blot. We detected expression of all the NS proteins in these cell lines as well as in original replicon cell (Huh-9-13) at almost at the same levels, although the levels of NS5A and NS5B in clone #6 were slightly low (Fig. 3). Interestingly, only clone #305 exhibited a different migration of NS5A, corresponding to the size of hyper-phosphorylated form (p58) in addition to the size of basal phosphorylated form (p56).

To analyze the change in IFNα signal transduction in two representative IFNα-resistant replicon cell lines (#8 and #305), we carried out a reporter gene assay using a firefly luciferase gene fused with three repeats of an ISG15-type IFN-stimulated responsive element (ISRE) as a reporter construct (pISRE/Luc). After transfection of pISRE/Luc to these replicon cells, the cells were stimulated with 1000 IU/mL of IFNα for 24 h. As shown in Fig. 4, the transactivation by IFNα in original replicon cells (Huh-9-13) was slightly reduced compared with that of parental cell line Huh-7 (Huh-7, 9.3-fold; Huh-9-13, 6.4-fold). Luciferase activity of #8 and #305 was more diminished than that of Huh-9-13 (#8, 3.6-fold; #305, 1.9-fold). The extent of decline of transactivation by IFNα treatment in these resistant replicon cell lines was dependent on the extent of IFNα-resistance, as quantified by RT-PCR (Fig. 2). It is suggested that the genetic alteration in HCV replicon RNA confers on IFNα-resistance in these cell lines.

In relation to the reporter gene analysis, JAK-STAT pathway activated by type I IFN was analyzed in IFNα-resistant replicons containing cells (#8 and #305). Phosphorylation of Stat-1, one of the important molecules in the JAK-STAT signal transduction pathway, was lowered in original replicon cells (Huh-9-13) compared with that in parental Huh-7 (Fig. 5A). However, severely impaired phosphorylation of Stat-1 was observed in the IFNα-resistant replicons containing cells (#8 and #305) compared with original replicon cells (Huh-9-13) (Fig. 5A). Furthermore, phosphorylation of Stat-1 was also decreased in #305 containing cells maintained in the absence of IFNα for 4 weeks, and the degree of decrease of Stat-1 phosphorylation was almost equal to that maintained in the presence of IFNα (data not shown). In contrast to these observations, Huh-7 cells, the parental cell of Huh-9-13 that was maintained in the presence of IFNα for 4 weeks did not show the significant alteration of Stat-1 phosphorylation compared with that maintained in the absence of IFNα (Fig. 5B). These results suggest that reduction of phosphorylation of Stat-1 in these IFNα-resistant replicon cell lines is caused by alteration of HCV replicon RNA and it may correlate with suppression of transcription from the reporter gene (Fig. 4).

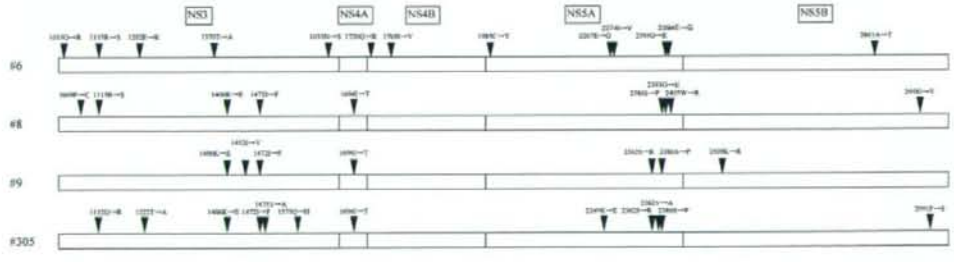

Fig. 8. The amino acid sequence deduced from nucleotide sequence in IFNα-resistant replicon cells. The nucleotide sequence was determined by an RT-PCR direct sequencing method. Arrows indicate the amino acid substitutions that were detected only in IFNα-resistant replicons compared with original replicon (Huh-9-13). The numbering of amino acids was referred to that of complete polyprotein of the isolate.

HCV replicon RNA confers IFNα-resistance

To confirm the role of HCV subgenomic RNA from clone #305 for acquisition of IFNα-resistance, total RNA was extracted from the cells and transfected to naive Huh-7 cells. The transfected cells were selected with G418 in the absence of IFNα. HCV negative-stranded replicon RNA, replication intermediate, and HCV NS proteins (NS3, NS5A and NS5B) were detected in the cells (data not shown).

Concerning the cells transfected with total RNA from IFNα-resistant #305 cell (#305/Huh-7) or the cells transfected with total RNA from original Huh-9-13 replicon cell (Huh-9-13/Huh-7), IFNα-sensitivity (EC_{50}) was analyzed (Fig. 6). IFNα-sensitivity (EC_{50}) of the Huh-9-13/Huh-7 showed 0.7 IU/mL, whereas the #305/Huh-7 showed 4.1 IU/mL. EC_{50} values of the Huh-7 cells bearing IFNα-resistant replicon derived from clone #305 were approximately 6-fold higher than that of Huh-7 cells bearing the original replicon. Although IFNα-resistance (EC_{50}) of the cells bearing #305 RNA was not as high as that of original #305, this finding suggests that acquisition of IFNα-resistance of these cells was due to genetic alteration of the replicon RNA.

We investigated the phosphorylation status of Stat-1 by stimulation of IFNα in these cells. As shown in Fig. 7, phosphorylation of Stat-1 in #305/Huh-7 (lane 2) was suppressed compared with that in Huh-9-13/Huh-7 (lane 4), suggesting that the IFNα-resistant HCV replicon derived from #305 is responsible for acquisition of the decreasing response to Stat-1 phosphorylation stimulated by IFNα.

Direct sequencing analysis of IFNα-resistant replicons

Nucleotide sequences in the NS region of each resistant clone were determined by RT-PCR direct sequencing. Sites of mutation that were detected only in IFNα-resistant replicons are shown by arrowheads and numbers (N-terminus of NS3 was denoted as 1027 based on the numbering of the complete polyprotein of the isolate), together with conversion of amino acids by arrows (Fig. 8). Although synonymous mutations are clustered in NS3 and the C-terminal region of NS5A, there were no common mutations among these resistant clones. Moreover, no mutations located at the positions as in IFNα-resistant replicons established by Namba et al. (2004) and Sumpter et al. (2004) were found in the present study. Mutations in the ISDR of NS5A were reported

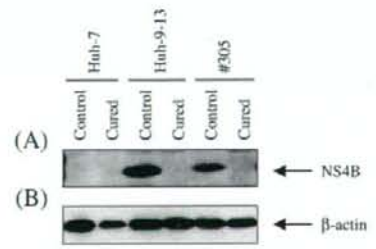

Fig. 9. Expression of NS protein (NS4B) (A) and β-actin (B) was confirmed in 'cured cells' by western blot analysis. Huh-7 cells with JTP-71892 as well as replicon cells (Huh-9-13 and #305) were analyzed likewise.

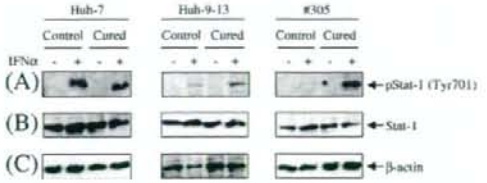

Fig. 10. Phosphorylation of Stat-1 (Tyr701) in 'cured cells'. Phosphorylation of Stat-1 (Tyr701) (A) by IFNα stimulation was investigated by western blot analysis. Stat-1 (B) and β-actin (C) were also analyzed. IFNα stimulation and western blot analysis were performed as described in Fig. 5.

to play an important role in outcome of IFN treatment to patients with genotype 1b of HCV in Japan (Enomoto et al., 1996); however, the amino acid sequence of ISDR was preserved among these replicon cell lines in our experiments.

Characterization of 'cured cells' obtained by IFNα-resistant HCV replicon cells

To clarify the role of HCV replicon RNA in resistance to IFNα, the replicon cells (Huh-9-13 and #305) were treated with JTP-71892 (1 μM) for more than 1 month to establish 'cured cells', as described in Materials and methods. JTP-71892 is a JTK-109-derivative synthesized in our laboratory, which has a potent inhibitory effect on HCV replication (Hirashima et al., 2006). The amounts of HCV replicon RNA in both replicon-bearing cell types were decreased less than what could be detected by quantitative RT-PCR, while the amounts of GAPDH mRNA used as a control did not show any difference (data not shown). The representative HCV NS protein, NS4B, was not detected in the 'cured cells' (Fig. 9).

The phosphorylation status of Stat-1 was then analyzed in these cells. The Stat-1 phosphorylation (Tyr701) by IFNα stimulation has restored remarkably in 'cured cells' (derived from both Huh-9-13 and #305) (Fig. 10). There was no obvious difference in the extent of Stat-1 phosphorylation by JTP-71892 treatment in Huh-7, indicating that restoration of Stat-1 phosphorylation was not due to JTP-71892. There was no clear difference in the amount of non-phosphorylated Stat-1 and β-actin expression by the IFNα stimulation or JTP-71892 treatment among these cell clones. These results suggest that HCV replicon RNA contributes to IFNα-resistance through impairment of phosphorylation of Stat-1, at least in part.

Discussion

We cultured HCV replicon cells in the presence of 10 and 30 IU/mL IFNα to isolate IFNα-resistant clones. Four different resistant clones with differing sensitivities to IFNα were isolated. The sensitivity for IFNα attenuated more than 100-fold in the #305 replicon, which was isolated in the presence of 30 IU/mL of IFNα and showed the most remarkable resistance in our study.

We analyzed the appearance of G418-resistant cells, #305/Huh-7, obtained by transfection of total RNA from the IFNα-

resistant replicon-bearing cells to Huh-7 by culturing them in the absence of IFNα, as shown in Fig. 1. IFNα sensitivities of the Huh-7 cells transduced with HCV replicon RNA of #305 cells were about 6-fold lower than those transfected with total RNA of original replicon cells (Huh-9-13), in coincident with a reduction of Stat-1 phosphorylation. However, #305/Huh-7 conferred a lesser extent of IFNα-resistance compared with that of parental #305 (Figs. 2 and 6). Although some factors other than HCV replicon RNA itself may participate in acquisition of IFNα-resistance in #305 cells, these results suggest that replicon RNA derived from #305 was significantly involved in regulation of IFNα signaling. The 'cured cells', from which HCV genomic RNA was removed from IFNα-resistant replicon cell line (#305) after treatment with 1 μM of JTP-71892, a potent HCV replication inhibitor, resulted in restoration of IFNα signaling to parental Huh-7. This finding suggests that HCV replicon RNA plays important roles in suppression of Stat-1 function. Moreover, this effect is dependent on mutation of HCV replicon RNA.

Mutations of amino acids were clustered throughout the whole region of NS3 and the C-terminus of NS5A in the IFNα-resistant replicon RNAs; however, there were no common amino acid mutations among the clones. This result may suggest the possibility that a change of plural functions participates in the acquisition of resistance. Whereas we did not identify common mutations, four amino acid mutations, K1406E, I1472F, I1694T, and S2386P, in NS3/4A and NS5A were shown to be common in #8, #9, and #305. In particular, the mutation at S2386P in NS5A located near region V3, one of the important prediction factors of the outcome in clinical IFN therapy (Nousbaum et al., 2000; Puig-Basagoiti et al., 2005), is found in #9 and #305. The nucleotide sequence of ISDR region was preserved between original replicon and IFNα-resistant replicons.

Concerning the mutations in NS5A region of #305, we established 3 chimeric replicon cell clones harboring Huh-9-13 replicon that was substituted with NS5A coding region derived from #305, which was selected by G418 in the absence of IFNα. These cell clones showed reduction of IFNα sensitivity (EC_{50}) as 20 to 30 times as those of normal replicon cell (Huh-9-13). Although chimeric replicons harboring #305 NS5A showed lesser extent of IFNα-resistance than that of #305 replicon cell, NS5A of #305 plays an important role in acquisition of IFNα-resistance in the replicon cell (data not shown).

Naka et al. (2005) reported that nonsense mutations and deletions of type I IFN receptor genes (IFNAR1, IFNAR2c) were found in certain clones of replicon cells that gained IFNα-resistance. However, we did not detect any such mutation or deletion in either of these genes in this work. Furthermore, we were not able to obtain resistant phenotype by IFN treatment at high concentrations of more than 1000 IU/mL.

In #305, among other IFNα-resistant clones, substantial amount of slow migrating form of NS5A was observed. From previous reports (Asabe et al., 1997, Ide et al., 1997; Kaneko et al., 1994; Kim et al., 1999; Reed et al., 1997, 1998; Tanji et al., 1995), it is supposed that this form is hyper-phosphorylated NS5A with 58 KD. Hyper-phosphorylated form of NS5A (p58) negatively participates in replication of HCV RNA in replicon cells (Appel et al., 2005; Evans et al., 2004; Huang et al., 2006; Neddermann et al., 2004). However, the quantity of basal HCV replication in #305 was almost the same as in other replicon cells, including Huh-9-13. Thus, it is likely that the hyper-phosphorylation of NS5A does not contribute to suppression of replication of HCV replicon. Rather, it may be related to a potent IFNα-resistance in #305 via un-identified mechanisms. Further studies are needed to clarify the role of hyper-phosphorylated NS5A in IFNα-resistance.

Concerning effects of NS5A on IFN signaling, it was reported that transiently- or stably-transfected NS5A inhibits IFN-stimulated Stat-1 phosphorylation and transactivation of ISRE in hepatocyte-derived cell lines, including Huh-7 cell (Gong et al., 2007; Lan et al., 2007). These authors also suggested the interaction of NS5A with Stat-1. Although these evaluation methods were different from that of our replicon system, they lend additional credibility to the suggestion that NS5A plays an important role in regulation of IFN signaling via inhibition of Stat-1 phosphorylation.

Stat-1 phosphorylation by IFNα stimulation was suppressed in IFNα-resistant replicon cells. The degree of suppression of Stat-1 phosphorylation was related to the sensitivity of IFNα in IFNα-resistant replicons (Fig. 5A). Moreover, the decrease of Stat-1 phosphorylation in #305 cells maintained in the absence of IFNα for 4 weeks was almost same level as that maintained in the presence of IFNα, suggesting that IFNα pressure did not induce a negative feedback (i.e. leading to the degradation of IFN receptor) loop in our experimental system. In contrast, Stat-1 phosphorylation was not changed significantly in parental Huh-7 cells that were maintained in the presence of IFNα compared with that maintained in the absence of IFNα (Fig. 5B), suggesting that Stat-1 phosphorylation in the parental Huh-7 cells was not affected with IFNα pressure and that the alteration of HCV replicon confers the IFNα-resistance. Stat-1 phosphorylation was also suppressed in the Huh-7 cells transfected with total RNA from IFNα-resistant replicon (Fig. 7). Moreover, the 'cured cells' showed a restoration of Stat-1 phosphorylation (Fig. 10). These observations suggest that IFNα-resistance in IFNα-resistant replicon cells depends on a change in Stat-1 phosphorylation, at least in part. For unknown reasons, we could not detect phosphorylation of Stat-2 (Tyr689), Stat-3 (Tyr705) (Sarcar et al., 2004; Zhu et al., 2005), JAK-1 (Tyr1022), or Tyk-2 (Tyr1054) in these cells. Concerning these proteins in the replicon cells, further investigation is needed to understand their roles in acquisition of IFNα-resistance.

Although the underlying mechanism of acquisition of IFNα-resistance gained by HCV replicon RNA remains unclear, clarification of detailed analysis of the role of Stat-1 in regard to IFN signaling in HCV replicon cells may contribute to the development therapeutic agents.

Materials and methods

Cell culture

Huh-9-13 cells harboring HCV subgenomic (NS3-3′X) replicon and parental Huh-7 cells were purchased from ReBLikon GmbH. Cells were cultured in Dulbecco's modified Eagle's

medium (DMEM) supplemented with 10% fetal bovine serum. To Huh-9-13 cells, 1 mg/mL of G418 (Geneticin; Invitrogen), a selective marker for replicated HCV subgenome was added.

IFN treatment

Huh-9-13 cells were seeded in a 75-cm^2 flask at a density of 3×10^5 cells/flask. Twenty-four hours after cell seeding, human IFNα (Sumiferon®300; Dainippon Sumitomo Pharma) was added so that the final concentration in medium was 10 IU/mL. Control cells were cultured in medium with no other additional substances. Cell passages were performed approximately every 7 days and the cells were cultured for approximately 1 month in the presence of IFNα (10 IU/mL). After decreases in sensitivity to IFNα were confirmed in the IFNα-treated groups by quantitative RT-PCR, IFNα-resistant cell phenotypes were further cultured for about 1 month in the presence of 30 IU/mL IFNα, and sensitivity to IFNα was then also measured in these cells. The cells cultured in the presence of 10 or 30 IU/mL of IFNα were cloned by a limiting dilution method using 96-well plates: cells were seeded at 1 cell/well and cultured in medium containing 10 IU/mL IFNα. After culture for about two to three weeks, survival and growth of cloned cells were confirmed, and then colonies were isolated and added to 48-well plates containing the test substance in 500 μL of culture medium per well. The proliferated cells in the 48-well plates were transferred to 6-well plates, and these were further put into 75-cm^2 cell culture flasks for subculture. Thereafter, subculture passage was performed approximately every 7 days. Cloning and subculture were performed in the presence of IFNα.

Measurement of IFN-sensitivity (quantitative analysis of HCV replicon and GAPDH mRNA)

IFN-sensitivity of IFNα-treated replicon cells was measured by quantitative RT-PCR. Cells (1×10^4 cells/well) were seeded in 96-well plates in the presence of 0, 0.1, 0.3, 1, 3, 10, 30, 100, 300, or 1000 IU/mL of IFNα. Forty-eight hours after cultivation with IFNα, the cells were harvested to extract total RNA using a total RNA extraction kit (RNeasy® 96; Qiagen) in accordance with the instruction manual. Quantification of HCV replicon RNA in the prepared RNA was performed using TaqMan® EZ RT-PCR Core Reagent (ABI) using a sequence detector under the following conditions: sense-primer: 5′-CGGGAGAGCCATAGTGG-3′ (130-S17; Greiner), antisense-primer: 5′-AGTACCACAAG-GCCTTTCG-3′ (290-R19; Greiner), probe: 5′(FAM)-CTGCG-GAACCGGTGAGTACAC (TAMRA)-3′ (148-S21FT; TaKaRa) (Takeuchi et al., 1999), RT-PCR reaction conditions: 50 °C, 2 min→60 °C, 30 min→95 °C, 5 min→45 cycles×(95 °C, 20 s→62 °C, 1 min). The number of copies in the samples was determined using a standard curve calibrated with 10^4 to 10^8 copies of synthesized HCV RNA standards encoding from 5′ terminus to E2 region, and recorded as amount of HCV RNA.

Direct sequencing analysis of HCV replicon RNA

Nucleotide sequences of HCV replicon RNA were analyzed by direct sequencing method. The NS region of total RNA extracted from IFNα-resistant replicon clones was divided into four fragments and amplified using an RT-PCR kit (ReverTra Dash®; TOYOBO). Four primers (HCV-NS-1RV: 5′-ATAGCACT-CGCACAGAACCGA-3′; Greiner, HCV-NS-2RV: 5′-GGAAC-CGTTTTTCACATGTCC-3′; Greiner, HCV-NS-3RV: 5′-ATGTGGTTAACGGCCTTGCT-3′; Greiner, HCV-NS-4RV: 5′-TCATCGGTTGGGGAGTAGATAGA-3′; Greiner) were used for reverse transcription (RT). For polymerase chain reaction (PCR), another four primers (HCV-NS-1FW: 5′-ATGGCGCC-TATTACGGCCTA-3′; Greiner, HCV-NS-2FW: 5′-TGTTC-GATTCCTCGGTTCTGT-3′; Greiner, HCV-NS-3FW: 5′-CCCCTTCTTCTCATGTCAACG-3′; Greiner, HCV-NS-4 FW: 5′-GGAACCTATCCAGCAAGCCC-3′; Greiner) were used in addition to the primers for RT.

RT and PCR reactions were conducted in accordance with the instruction manual provided with the kit. RT reaction was conducted at 42 °C, 20 min, and the reaction mixtures were then heated to 99 °C, 5 min. The PCR reaction was performed for 30 cycles under the following conditions: 98 °C, 10 s; 60 °C, 2 s; then 74 °C, 90 s.

Sequencing was performed using a BigDye Terminator Cycle Sequencing Ready Reaction Kit (ABI). One μL of amplified RT-PCR product for each clone was purified using QIAquick Gel Extraction kit (Qiagen) and the sequence primers were used to prepare each of the reaction solutions in accordance with the manufacturer's procedure. Twenty μL of each solution was allowed to react for 25 cycles under the conditions: 96 °C, 10 s; 50 °C, 5 s; 60 °C, 4 min; then 72 °C, 7 min. The solutions were then purified by Dye EX 2.0 (Qiagen) in accordance with the instruction manual. After that, the samples were applied for sequencing analysis using an ABI PRISM 3100 genetic analyzer (ABI).

The NS region (5952 bp, 1984 amino acids) in sequenced samples underwent gene analysis using Vector NTI analysis software (Invitrogen). In a comparison of deduced amino acid sequences based on nucleotide sequences among the four IFNα-resistant replicon clones and original replicons, the NS regions were compared to that of the original replicon clone to identify mutations. The amino acid sequence of the original replicon cells was included among the materials provided with the Huh-9-13 cell line product from ReBLikon GmbH.

Reporter gene analysis

We attempted to clarify IFNα transactivation in IFNα-resistant replicons. Firefly luciferase fused gene with three repeats of an ISG15-type IFN-stimulated responsive element (ISRE) was used as a reporter construct (pISRE/Luc). HCV replicon cells or Huh-7 cells (3×10^5 cells/well) were seeded on a 60-mm plate in the absence of IFNα. Eight hours after cell seeding, the reporter construct (3 μg) was transfected using FuGENE6 (Roche) as a transfection reagent, following the instruction manual. The transfected cells were cultured further 12 to 14 h, and then the cells (1×10^4 cells) were inoculated on a 96-well plate and cultured for 24 h with or without 1000 IU/mL of IFNα. The luciferase activity was measured by adding Steady Glo® to the cells using TopCount (Packard).

Western blot analysis

The cell lysates were prepared in Laemmli buffer (BIO-RAD) and subjected to SDS-2/15% gradient PAGE and transferred onto nitrocellulose membranes. To detect expression of HCV NS proteins, antibodies against NS3, NS4B, NS5A, and NS5B were used. Anti-β-actin antibody (Sigma) was also used for detection of β-actin as an internal control.

To investigate the phosphorylation of Stat-1 at Tyr701 in HCV replicon cells and its parental Huh-7 cells, the cells were cultured in the medium containing 500 IU/mL of IFNα for 30 min. After cell lysates were prepared as previously described, western blot analysis was performed using an anti-phospho-Stat-1 (Tyr701) antibody (Cell Signaling Technology) or an anti-Stat-1 antibody (BD Transduction Laboratories). Immunocomplexes were detected by visualization using enhanced chemiluminescence (Amersham Biosciences).

Transfection of total RNA derived from replicon cells to naive Huh-7

Total RNA (5 μg) extracted from HCV replicon cells was transfected to Huh-7 cells using DMRIE-C transfection reagents, in accordance with the instruction manuals provided with the reagents. The transfected cells were cultured in the absence of IFNα and selected with 1000 μg/mL of G418 for 4 weeks. Drug-resistant cells were collected and reactivity to IFNα was measured as described in previous section.

Elimination of HCV replicon RNA from replicon cells (Isolation of 'cured' replicon)

To remove HCV replicon RNA from replicon cells, HCV replicon cells were treated ('cured') with HCV RNA-dependent RNA polymerase NS5B inhibitor, JTP-71892, JTK-109-derivatives synthesized in our laboratory (Hirashima et al., 2006; Ishida et al., 2006). The replicon cells (5×10^4 cells) were inoculated on a 60-mm plate and further cultured in the presence of the compound (1 μM) for about 4 weeks. The cell culture was performed in the absence of G418, to prevent survival of the compound-resistant clones. Medium was exchanged with fresh medium containing the compound twice per week. The finding that 1 μM of JTP-71892 does not exhibit any toxicity or growth inhibition in long-term culture had been previously confirmed.

Acknowledgments

We thank M. Tomonaga, Y. Hori and K. Asahina for their technical assistance in this work. We also greatly acknowledge Dr. R. Bartenschlager for providing us the HCV subgenomic replicon (Huh-9-13) and naive Huh-7 cell lines for parental cell line of Huh-9-13.

References

Alter, M.J., 1997. Epidemiology of hepatitis C. Hepatology 26, 62S–65S.

Appel, N., Pietschmann, T., Bartenschlager, R., 2005. Mutational analysis of hepatitis C virus nonstructural protein 5A: potential role of differential phosphorylation in RNA replication and identification of a genetically flexible domain. J. Virol. 79, 3187–3194.

Asabe, S., Tanji, Y., Satoh, S., Kaneko, T., Kimura, K., Shimotohno, K., 1997. The N-terminal region of hepatitis C virus-encoded NS5A is important for NS4A dependent phosphorylation. J. Virol. 71, 790–796.

Bartenschlager, R., Lohmann, V., 2000. Replication of hepatitis C virus. J. Gen. Virol. 81, 1631–1648.

Bartenschlager, R., Lohmann, V., 2001. Novel cell culture systems for the hepatitis C virus. Antivir. Res. 52, 1–17.

Choo, Q.L., Richman, K.H., Han, J.H., Berger, K., Lee, C., Dong, C., Gallegos, C., Coit, D., Medina, S.R., Barr, P.J., Weiner, A.J., Bradely, D.W., Kuo, G., Houghton, M., 1991. Genetic organization and diversity of the hepatitis C virus. Proc. Natl. Acad. Sci. U. S. A. 88, 2451–2455.

Enomoto, N., Sakuma, I., Asahina, Y., Kurosaki, M., Murakami, T., Yamamoto, C., Ogura, Y., Izumi, N., Marumo, F., Sato, C., 1996. Mutations in the nonstructural protein 5A gene and response to interferon I patients with chronic hepatitis C virus 1b infection. N. Engl. J. Med. 334, 77–81.

Evans, M.J., Rice, C.M., Goff, S.P., 2004. Phosphorylation of hepatitis C virus nonstructural protein 5A modulates its protein interactions and viral RNA replication. Proc. Natl. Acad. Sci. U. S. A. 101, 13038–13043.

Frese, M., Schwärzle, V., Barth, K., Krieger, N., Lohmann, V., Mihm, S., Haller, O., Bartenschlager, R., 2002. Interferon-γ inhibits replication of subgenomic and genomic hepatitis C virus RNAs. Hepatology 35, 694–703.

Gale, M.J., Korth, M.J., Tang, N.M., Tan, S.L., Hopkins, D.A., Dever, T.E., Polyak, S.J., Gretch, D.R., Katze, M.G., 1997. Evidence that hepatitis C virus resistance to interferon is mediated through repression of the PKR protein kinase by nonstructural 5A protein. Virology 230, 217–227.

Gong, G.Z., Cao, J., Jiang, Y.F., Zhou, Y., Liu, B., 2007. Hepatitis C virus nonstructural 5A abrogates signal transducer and activator of transcription-1 nuclear translocation induced by IFN-alpha through dephosphorylation. World Gastroenterol. 13, 4080–4084.

Guo, J.T., Bichko, V.V., Seeger, C., 2001. Effect of alpha interferon on the hepatitis C virus replicon. J. Virol. 75, 8516–8523.

Guo, J.T., Sohn, J.A., Zhu, Q., Seeger, C., 2004. Mechanism of the interferon alpha response against hepatitis C virus replicons. Virology 325, 71–81.

Hijikata, M., Kato, N., Ootsuyama, Y., Nakagawa, M., Shimotohno, K., 1991. Gene mapping of the putative structural region of the hepatitis C virus genome by *in vitro* processing analysis. Proc. Natl. Acad. Sci. U. S. A. 88, 5547–5551.

Hijikata, M., Mizushima, H., Tanji, Y., Komoda, Y., Hirowatari, Y., Akagi, N., Kato, N., Kimura, K., Shimotohno, K., 1993a. Proteolytic processing and membrane association of putative nonstructural proteins of hepatitis C virus. Proc. Natl. Acad. Sci. U. S. A. 90, 10773–10777.

Hijikata, M., Mizushima, H., Tanji, Y., Komoda, Y., Hirowatari, Y., Akagi, N., Kato, N., Kimura, K., Shimotohno, K., 1993b. Two distinct proteinase activities required for the processing of a putative nonstructural precursor protein of hepatitis C virus. J. Virol. 67, 4665–4675.

Hirashima, S., Suzuki, T., Ishida, T., Noji, S., Yata, S., Ando, I., Komatsu, M., Ikeda, S., Hashimoto, H., 2006. Benzimidazole derivatives bearing substituted biphenyls as hepatitis C virus NS5B RNA-dependent RNA polymerase inhibitors: structure-activity relationship studies and identification of a potent and highly selective inhibitor JTK-109. J. Med. Chem. 49, 4721–4736.

Houghton, M., 1996. Hepatitis C viruses, p1035–1058, In: Fields, B.N., Knipe, D.M., Howley, P.M. (Eds.), Fields Virology, 3rd ed. Lippincott-Raven Co., Philadelphia.

Huang, Y., Chen, X.C., Konduri, M., Fomina, N., Lu, J., Jin, L., Kolykhalov, A., Tan, S.L., 2006. Mechanistic link between the anti-HCV effect of interferon gamma and control of viral replication by a Ras-MAPK signaling cascade. Hepatology 43, 81–90.

Ide, Y., Tanimoto, A., Sasaguri, Y., Padmanabhan, R., 1997. Hepatitis C virus NS5A protein is phosphorylated in vitro by a stably bound protein kinase from HeLa cells and by cAMP-dependent protein kinase A-a catalytic subunit. Gene 201, 151–158.

Ishida, T., Suzuki, T., Hirashima, S., Mizutani, K., Yoshida, A., Ando, I., Ikeda, S., Adachi, T., Hashimoto, H., 2006. Benzimidazole inhibitors of hepatitis C

virus NS5B polymerase: identification of 2-[(4-diarylmethoxy) phenyl]-benzimidazole. Bioorg. Med. Chem. Lett. 16, 1859–1863.
Kaneko, T., Tanji, Y., Satoh, S., Hijikata, M., Asabe, S., Kimura, K., Shimotohno, K., 1994. Production of two phosphoproteins from the NS5A region of the hepatitis C virus genome. Biochem. Biophys. Res. Commun. 205, 320–326.
Kato, N., Hijikata, M., Ootsuyama, M., Nakagawa, S., Ohkoshi, S., Sugimura, T., Shimotohno, K., 1990. Molecular cloning of the human hepatitis C virus genome from Japanese patients with non-A, non-B hepatitis. Proc. Natl. Acad. Sci. U. S. A. 87, 9524–9528.
Kawai, T., Takahashi, K., Sato, S., Coban, C., Kumar, H., Kato, H., Ishii, K.J., Takeuchi, O., Akira, S., 2005. IPS-1, an adaptor triggering RIG-I- and Mda5-mediated type I interferon induction. Nat. Immunol. 6, 1074–1076.
Kim, J., Lee, D., Choe, J., 1999. Hepatitis C virus NS5A protein is phosphorylated by casein kinase II. Biochem. Biophys. Res. Commun. 257, 777–781.
Lan, K.H., Lan, K.L., Lee, W.P., Sheu, M.L., Chen, M.Y., Lee, Y.L., Yen, S.H., Chang, F.Y., Lee, S.D., 2007. HCV NS5A inhibits interferon-alpha signaling through suppression of STAT1 phosphorylation in hepatocyte-derived cell lines. J. Hepatol. 46, 759–767.
Lindsay, K.L., 1997. Therapy of hepatitis C: overview. Hepatology 26, 71S–77S.
Lohmann, V., Körner, F., Koch, J., Herian, U., Theilman, L., Bartenschlager, R., 1999. Replication of subgenomic Hepatitis C virus RNAs in a hepatoma cell line. Science 285, 110–113.
McHutchison, J.G., Gordon, S.C., Schiff, E.R., Shiffman, M.L., Lee, W.M., Rustgi, V.K., Goodman, Z.D., Ling, M.H., Cort, S., Albrecht, J.K., 1998. Interferon alfa-2b alone or in combination with ribavirin as initial treatment for chronic hepatitis C. Hepatitis Interventional Therapy Group. N. Engl. J. Med. 339, 1485–1492.
Meylan, E., Curran, J., Hofmann, K., Moradpour, D., Binder, M., Bartenschlager, R., Tschopp, J., 2005. Cardif is an adaptor protein in the RIG-I antiviral pathway and is targeted by hepatitis C virus. Nature 437, 1167–1172.
Naka, K., Takemoto, K., Abe, K., Dansako, H., Ikeda, M., Shimotohno, K., Kato, N., 2005. Interferon resistance of hepatitis C virus replicon-harboring cells is caused by functional disruption of type I interferon receptors. J. Gen. Virol. 86, 2787–2792.
Namba, K., Naka, K., Dansako, H., Nozaki, A., Ikeda, M., Shiratori, Y., Shimotohno, K., Kato, N., 2004. Establishment of hepatitis C virus replicon cell lines possessing interferon-resistant phenotype. Biochem. Biophys. Res. Commun. 323, 299–309.
Neddermann, P., Quintavalle, M., Di Pietro, C., Clementi, A., Cerretani, M., Altamura, S., Bartholomew, L., De Francesco, R., 2004. Reduction of hepatitis C virus NS5A hyperphosphorylation by selective inhibition of cellular kinases activates viral RNA replication in cell culture. J. Virol. 78, 13306–13314.
Noguchi, T., Satoh, S., Noshi, T., Hatada, E., Fukuda, R., Kawai, A., Ikeda, S., Hijikata, M., Shimotohno, K., 2001. Effects of mutation in hepatitis C virus nonstructural protein 5A on interferon resistance mediated by inhibition of PKR kinase activity in mammalian cells. Microbiol. Immunol. 45, 829–840.
Nousbaum, J., Polyak, S.J., Ray, S.C., Sullivan, D.G., Larson, A.M., Caritherns, R.L., Gretch, D.R., 2000. Prospective characterization of full-length hepatitis C virus NS5A quasispecies during induction and combination antiviral therapy. J. Virol. 74, 9028–9038.
Okamoto, H., Okada, S., Sugiyama, Y., Kurai, K., Iizuka, H., Machida, A., Miyakawa, Y., Tsuda, F., Mayumi, M., 1991. Nucleotide sequence of the genomic of hepatitis C virus isolated from a human carrier: comparison with reported isolates for conserved and divergent regions. J. Gen. Virol. 72, 2697–2704.
Okamoto, H., Kurai, K., Okada, S., Yamamoto, K., Iizuka, H., Tanaka, T., Fukuda, S., Tsuda, F., Mishiro, S., 1992. Full-length sequence of a hepatitis C virus genome having poor homology to reported isolates: comparative study of four distinct genotypes. Virology 188, 331–341.
Puig-Basagoiti, F., Forns, X., Furcic, I., Ampurdanes, S., Gimenez-Barcons, M., Franco, S., Sanchez-Tapias, J.M., Saiz, J.C., 2005. Dynamics of hepatitis C virus NS5A quasispecies during interferon and ribavirin therapy in responder and non-responder patients with genotype 1b chronic hepatitis C. J. Gen. Virol. 86, 1067–1075.
Reed, K.E., Xu, J., Rice, C.M., 1997. Phosphorylation of the hepatitis C virus NS5A protein in vitro and in vivo: properties of the NS5A-associated kinase. J. Virol. 71, 7187–7197.
Reed, K.E., Gorbalenya, A.E., Rice, C.M., 1998. The NS5A/NS5 proteins of viruses from three genera of the family *Flaviviridae* are phosphorylated by associated serine/threonine kinases. J. Virol. 72, 6199–6206.
Sarcar, B., Ghosh, A.K., Steele, R., Ray, R., Ray, R.B., 2004. Hepatitis C virus NS5A mediated STAT3 activation requires co-operation of Jak1 kinase. Virology 322, 51–60.
Seth, R.B., Sun, L., Ea, C.K., Chen, Z.J., 2005. Identification and characterization of MAVS, a mitochondrial antiviral signaling protein that activates NF-kappaB and IRF 3. Cell 122, 669–682.
Sumpter Jr., R., Wang, C., Foy, E., Loo, Y.M., Gale Jr., M., 2004. Viral evolution and interferon resistance of hepatitis C virus RNA replication in a cell culture model. J. Virol. 78, 11591–11604.
Taguchi, T., Nagano-Fujii, M., Akutsu, M., Kadoya, H., Ohgimoto, S., Ishido, S., Hotta, H., 2004. Hepatitis C virus NS5A protein interacts with 2′, 5′-oligoadenylate synthetase and inhibits antiviral activity of IFN in an IFN sensitivity-determining region-independent manner. J. Gen. Virol. 85, 959–969.
Takamizawa, A., Mori, C., Fuke, I., Manabe, S., Murakami, S., Fujita, J., Onishi, E., Andoh, T., Yoshida, I., Okayama, H., 1991. Structure and organization of the hepatitis C virus genome isolated from human carriers. J. Virol. 65, 1105–1113.
Takeuchi, T., Katsume, A., Tanaka, T., Abe, A., Inoue, K., Tsukiyama-Kohara, K., Kawaguchi, R., Tanaka, S., Kohara, M., 1999. Real-time detection system for quantification of hepatitis C virus genome. Gastroenterology 116, 636–642.
Tanji, Y., Kaneko, T., Satoh, S., Shimotohno, K., 1995. Phosphorylation of hepatitis C virus-encoded nonstructural protein NS5A. J. Virol. 69, 3980–3986.
Tong, C.Y., Gilmore, I.T., Hart, C.A., 1995. HCV-associated liver cancer. Lancet 345, 1058–1059.
Xu, L.G., Wang, Y.Y., Han, K.J., Li, L.Y., Zhai, Z., Shu, H.B., 2005. VISA is an adapter protein required for virus-triggered IFN-beta signaling. Mol. Cell 19, 727–740.
Yoneyama, M., Kikuchi, M., Natsukawa, T., Shinobu, N., Imaizumi, T., Miyagishi, M., Taira, K., Akira, S., Fujita, T., 2004. The RNA helicase RIG-I has an essential function in double-stranded RNA-induced innate antiviral responses. Nat. Immunol. 5, 730–737.
Zhu, H.m., Nelson, D.R., Crawford, J.M., Liu, C., 2005. Defective Jak-Stat activation in hepatoma cells is associated with hepatitis C viral IFN-alpha resistance. J. Interferon Cytokine Res. 25, 528–539.

Biochemical and Biophysical Research Communications 379 (2009) 330–334

Contents lists available at ScienceDirect

Biochemical and Biophysical Research Communications

journal homepage: www.elsevier.com/locate/ybbrc

3D cultured immortalized human hepatocytes useful to develop drugs for blood-borne HCV

Hussein Hassan Aly [a], Kunitada Shimotohno [b], Makoto Hijikata [a,c,*]

[a] Laboratory of Human Tumor Viruses, The Institute for Virus Research, Kyoto University, Department of Viral Oncology, 53 Kawaharacho, Shogoin, Sakyoku, Kyoto 606-8507, Japan
[b] Center for Human Metabolomic Systems Biology, Keio University, 35 Shinano-machi, Shinjuku-ku, Tokyo 160-8582, Japan
[c] Laboratory of Viral Oncology, Graduate School of Biostudies, Kyoto University, Konoecho, Yoshida, Sakyoku, Kyoto 606-8501, Japan

ARTICLE INFO

Article history:
Received 5 December 2008
Available online 25 December 2008

Keywords:
Hepatitis C virus
Infection
Replication
3D culture
PPAR
Immortalized hepatocytes
Blood-borne HCV

ABSTRACT

Due to the high polymorphism of natural hepatitis C virus (HCV) variants, existing recombinant HCV replication models have failed to be effective in developing effective anti-HCV agents. In the current study, we describe an *in vitro* system that supports the infection and replication of natural HCV from patient blood using an immortalized primary human hepatocyte cell line cultured in a three-dimensional (3D) culture system. Comparison of the gene expression profile of cells cultured in the 3D system to those cultured in the existing 2D system demonstrated an up-regulation of several genes activated by peroxisome proliferator-activated receptor alpha (PPARα) signaling. Furthermore, using PPARα agonists and antagonists, we also analyzed the effect of PPARα signaling on the modulation of HCV replication using this system. The 3D *in vitro* system described in this study provides significant insight into the search for novel anti-HCV strategies that are specific to various strains of HCV.

Infection with Hepatitis C virus (HCV) is a serious health problem worldwide and leads to high rates of liver cirrhosis and hepatocellular carcinoma [1]. Given that the standard HCV therapy remains insufficient for the successful treatment of many patients [2], the development of more effective and less toxic anti-HCV agents is required. *In vitro* systems like the HCV replicon-bearing cells and the infectious particle-producing JFH1 system, has contributed to the discovery of new targets for anti-HCV therapy. However, these recombinant HCV genomes only proliferate in sublines of HuH-7 cells, which do not permit infection or proliferation of blood-borne HCV. Due to the high polymorphism of natural HCV, data from recombinant HCV systems could be evaluated by studying the therapeutic response of a variety of naturally occurring HCVs. However, the current systems available for such study remain insufficient due to the low infection and replication efficiency of the natural HCV strains.

More recently, production and secretion of infectious HCV particles has been reported in two independent three-dimensional (3D) cell culture systems, termed the radial-flow bioreactor (3D/RFB) and the thermoreversible gelatin polymer (3D/TGP) systems. These results were not observed in monolayer cultures [3], suggesting that hepatocytes cultured in 3D more closely resemble liver cells *in vivo* [4] and thus support HCV proliferation. In addition, analysis of gene expression levels in 3D cultured cells revealed that the newly established immortalized human hepatocyte (HuS-E/2 cells) gene profile was altered to more closely resemble that of human liver tissue when the cells were cultured in 3D/TGP [5].

In the current study, we cultured HuS-E/2 cells in 3D/TGP and demonstrated efficient proliferation of natural HCV. Furthermore, gene expression analysis of these cells demonstrated the activation of the peroxisome proliferators-activated receptor α (PPARα) signaling pathway, suggesting an important role for this pathway in the replication of natural HCV. Thus, the *in vitro* system described appears to be a useful tool for the study of HCV infection and proliferation as well as for the development of effective anti-viral agents against various natural HCVs.

Materials and methods

Cell culture. Immortalized human hepatocytes (HuS-E/2) and LucNeo#2 replicon cells [6] were cultured as previously described [5,7]. For the 3D-TGP culture system, 1×10^5 HuS-E/2 cells were cultured in 1 ml Mebiol gel (Mebiol Inc., Kanagawa, Japan)/well in 12-well plates. Five hundred microliters of fresh medium was overlaid on the solidified gel, and was changed every 2 days. Cell

* Corresponding author. Address: Laboratory of Human Tumor Viruses, The Institute for Virus, Kyoto University, Department of Viral Oncology, 53 Kawaharacho, Shogoin, Sakyoku, Kyoto 606-8507, Japan. Fax: +81 75 751 3998.
E-mail address: mhijikat@virus.kyoto-u.ac.jp (M. Hijikata).

0006-291X/$ - see front matter © 2008 Elsevier Inc. All rights reserved.
doi:10.1016/j.bbrc.2008.12.054

extraction from the gel was done at the designated time points according to the manufacturer's protocol.

RNA extraction, reverse transcriptase polymerase chain reaction (RT-PCR) and real-time RT-PCR (Q-PCR). At the designated time points, total cellular RNA was extracted and 1 μg of total RNA was used as a template for RT-PCR and for the quantitative detection of HCV-RNA using real-time RT-PCR (Q-PCR) as previously described [10].

HCV infection experiment. HCV infection experiments were carried out using sera from patients infected with HCV. Infection in 2D culture was undertaken as previously described [5]. For 3D/TGP cultured cells, the gel was solidified, and 50 μl HCV-containing patient serum with a titer of 1×10^6 HCV-RNA/ml was added to the culture and mixed. The culture was continued until the cells were extracted. Following extraction from 3D-TGP, cells were centrifuged and washed three times thoroughly with PBS. RNA was then extracted from the cells as described above. HCV infection into HuS-E/2 cells was also examined in the presence of anti-E2 mouse monoclonal antibody (917) as outlined previously [8].

Treatment of cells with PPARα signaling agonists and antagonists. Fenofibrate or MK886 (Sigma–Aldrich, USA) were added to the culture medium of HuS-E/2 (2D-HuS-E/2) cells from day 0 of HCV infection; or the culture medium of LucNeo#2 replicon harboring cells. The cells were then cultured to the designated time point.

Microarray analysis. Gene expression profiles of 3D/TGP cultured HuS-E/2 cells were obtained by microarray analysis (3D-Genes Human 25, Toray, Tokyo, Japan) and compared to those of cells cultured in 2D.

Results

3D/TGP cultures enhance HCV proliferation in HuS-E/2 cells

Infection and proliferation of the HCV genotype 1b (HCV-RC5) derived from the serum of patient RC5 in HuS-E/2 cells cultured in 3D/TGP (3D/TGP-HuS-E/2 cells) was investigated and compared with that of HuS-E/2 cells cultured in 2D (2D-Hus-E/2). As outlined in Fig. 1A, the HCV-RNA levels in the 3D/TGP-HuS-E/2 cells were significantly higher at all of the time points examined following infection than in the 2D-HuS/E2 cells, suggesting that the 3D/TGP system greatly enhances the proliferation of naturally occurring HCV in HuS-E/2 cells. Similar results were also obtained for sera from additional patients (data not shown). To examine whether the infection is viral envelope-receptor mediated, the infection experiments using serum treated with anti-HCV-E2 antibody (α-E2) or with anti-tubulin (negative control) was also performed. Pre-incubation of the serum with α-E2 significantly reduced the total amount of HCV-RNA in the cells upon infection (Fig. 1B). This result suggested that the infection of natural HCV into 3D/TGP-HuS-E/2 cells was HCV-E2-dependent.

Inhibition of natural HCV replication in HuS-E/2 cells by Interferon

In order to test the effects of anti-viral agents on natural HCV replication in 3D/TGP HuS-E/2 cells, 50–100 U/ml of IFNα was added to the medium overlaying the HCV-RC5 infected 3D/TGP-HuS-E/2 cells. The two treatment concentrations resulted in the inhibition of HCV-RNA replication in 3D-HuS-E/2 cells by

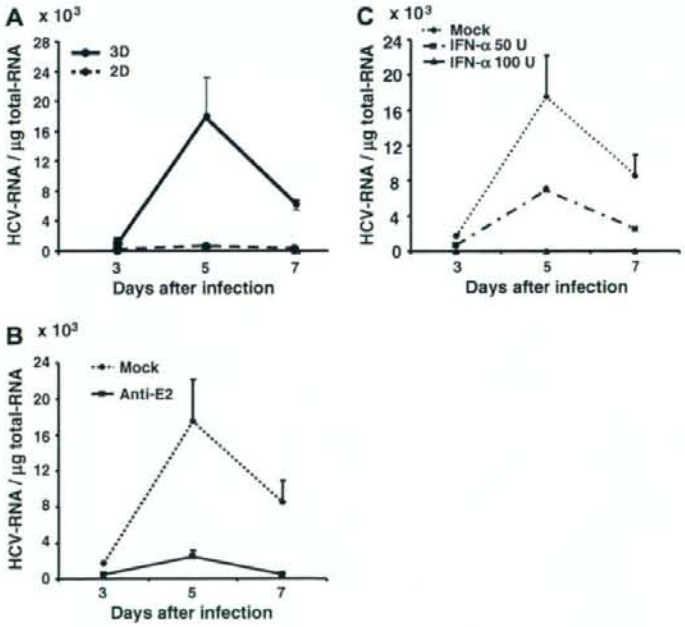

Fig. 1. HCV infection into 3D/TGP-HuS-E/2 cells. (A) 3D/TGP significantly enhanced HCV proliferation in HuS-E/2 cells. HCV patient serum was used to infect a similar number of HuS-E/2 cells cultured in 2D (hashed line) or 3D/TGP (solid line) culture for 24 h. Cells were then harvested and lysed at the indicated time points (3–7 days). The quantity of genomic HCV-RNA per 1 μg total RNA was determined by Q-PCR analysis. (B) Anti-E2 antibodies blocked HCV infection. HCV infection was performed as described in panel A in the presence of Anti-E2 specific or anti-tubulin (control) antibodies. (C) IFNα inhibits HCV replication in 3D/TGP-HuS-E/2 cells. HuS-E/2 cells were infected with HCV and fresh medium supplemented with or without (Mock), 50 U/ml, or 100 U/ml IFNα overlaid on the gel containing the cells and HCV proliferation measured as described above.

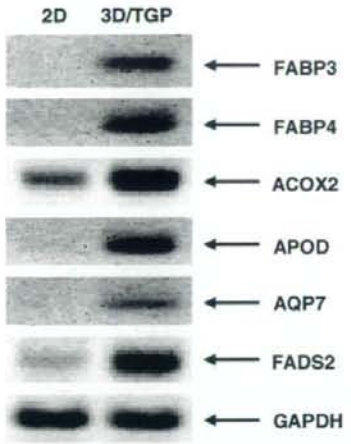

Fig. 2. RT-PCR analysis of the expression of genes identified by microarray. The PPARα regulated genes were increased in 3D/TGP-HuS-E/2 cells (3D-TGP) and their expression levels measured by RT-PCR. 2D represents RNA samples from 2D-HuS-E/2 cells. Twenty cycles of amplification were undertaken for the RT-PCR analysis. GAPDH expression served as an internal control. *Abbreviations:* FABP3, fatty acid binding proteins 3; FABP4, fatty acid binding proteins 4; ACOX2, acyl-coenzyme A oxidase 2; APOD, apolipoprotein D; AQP7, aquaporin 7; FADS2, fatty acid desaturase 2; GAPDH, glyceraldehyde 3-phosphate dehydrogenase.

approximately 50–60% and almost completely, respectively, when compared to the replication in cells receiving mock treatment (Fig. 1C). These results demonstrate that the IFNα treatment was effective on HCV derived from RC5 and that 3D/TGP-HuS-E/2 cells may be useful for the screening of anti-HCV drugs for the treatment of natural HCV.

Increased activation of the PPARα signaling pathway in 3D cultured HuS-E/2 cells

Given that 3D/TGP-HuS-E/2 cells demonstrated enhanced proliferation of natural HCV, the gene expression profiles of these cells was compared with that of cells cultured under normal 2D conditions using microarray analysis in order to identify the factors required for the enhanced proliferation. Among the 24,268 genes compared in this analysis, 212 genes demonstrated a greater than four folds index increase in expression in 3D/TGP than standard cultured cells. Cell signaling pathway analysis of these 212 genes showed that six genes, including fatty acid binding proteins 4 and 3 (FABP4 and 3), apolipoprotein D (APOD), aquaporin 7 (AQP7), acyl-coenzyme A oxidase 2 (ACOX2), and fatty acid desaturase 2 (FADS2), were targets of PPARα signaling [9–12]. The increased expression of these genes in the 3D/TGP-HuS-E/2 cells was further confirmed by RT-PCR analysis (Fig. 2). Given that PPARα is an essential factor for normal hepatocyte function [13], these results indicate that 3D/TGP culture enhances the hepatocyte-specific characteristics of HuS-E/2 cells.

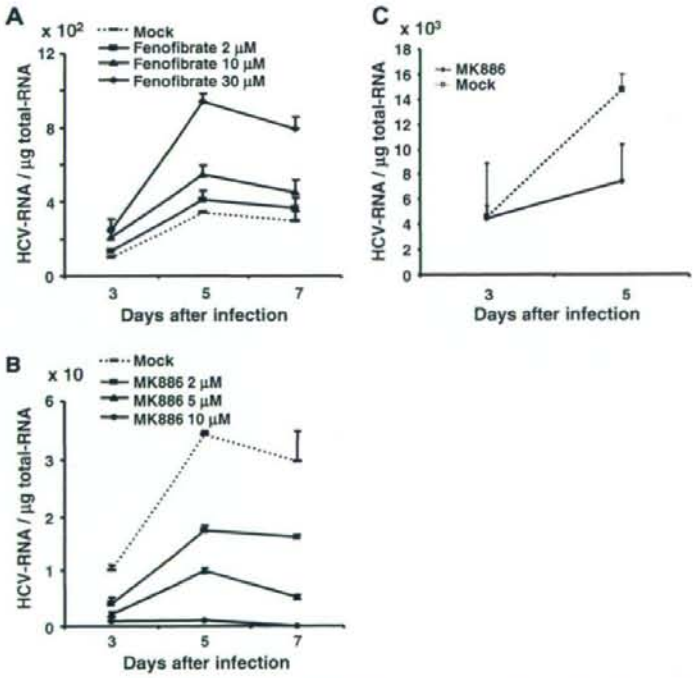

Fig. 3. The effects of PPARα agonists and antagonists on natural HCV proliferation. (A) HuS-E/2 cells were infected with HCV and fresh medium supplemented with or without (Mock) 2, 10, or 30 μM of fenofibrate overlaid on the cells. (B) Medium supplemented with or without (Mock), 2, 5, or 10 μM of MK886 was overlaid on 2D-HuS-E/2 cells infected with HCV. HCV proliferation following treatment was measured by Q-PCR. (C) Medium supplemented with or without (Mock), 10 μM of MK886 was overlaid on 3D/TGP-HuS-E/2 cells infected with HCV. HCV proliferation following treatment was measured by Q-PCR.

PPARα signaling affects HCV replication

We next examined the potential role of PPARα signaling on HCV proliferation by monitoring HCV replication in 2D-HuS-E/2 cells that had been infected with HCV-RC5 and subsequently treated with the PPARα agonist fenofibrate [14] or the PPARα antagonist MK886 [14] (Fig. 3B). As outlined in Fig. 3A, a dose-dependent increase in HCV replication was observed in fenofibrate-treated cells. In contrast, a dose-dependent decrease in HCV proliferation was observed in the presence of MK886. Similarly, treatment with MK886 reduced HCV proliferation in 3D/TGP-HuS-E/2 cells (Fig. 3C). The response of HCV proliferation in response to fenofibrate and MK886 treatment was also analyzed in LucNeo#2 cells that contained HCV replicon RNA (LNMH14) derived from the HCV-1b genome (Fig. 4A). Luciferase expression in these cells represented replication of the HCV replicon [6] and, as shown in Fig. 4A, luciferase activity in the cells treated with fenofibrate or MK886 also showed either enhancement or suppression of replicon proliferation, respectively. In addition, the increased HCV replication following fenofibrate treatment was completely abolished when treated with MK886 simultaneously. As MK886 is known to induce apoptosis when administered in high doses [15], the cell viability was examined using the XTT assay. There were no significant effects on cell viability after treatment with fenofibrate. Although MK886 resulted in a minor reduction in XTT values when high doses (10–15 μM) were administered, this reduction was not statistically significant when compared to its effect on HCV replication (Fig. 4B). This result suggests that PPARα signaling is required for HCV replication and that suppression of PPARα signaling has an anti-HCV effect.

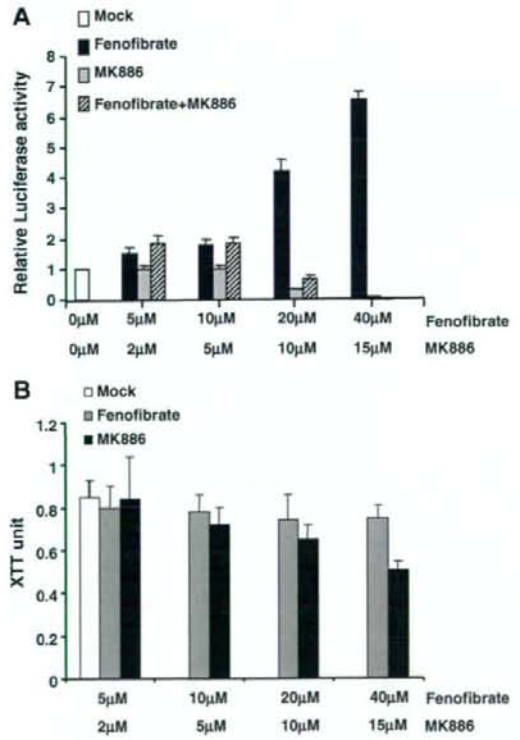

Fig. 4. The effects of PPARα agonists and antagonists on the replication of HCV subgenomic replicons. (A) LucNeo#2 cells containing a HCV subgenomic replicon termed LNMH14, were mock treated or treated with fenofibrate, MK886, or a combination of both fenofibrate and MK886 at the indicated concentrations for 2 days. Luciferase activity derived from the replicon was then measured as an indicator of HCV replication [7]. (B) Following treatment with fenofibrate and Mk886, LucNeo#2 cells were cultured for 2 days and cell viability measured using the XTT assay (Roche, Mannheim, Germany).

Discussion

In the current study, we demonstrated that immortalized hepatocyte HuS-E/2 cells cultured in 3D/TGP support the infection and replication of natural HCV derived from patient sera. Unlike recombinant HCVs, which have been required to adapt to sublines of HuH-7 cells [16], the population of the natural HCV is fairly polymorphic, demonstrating different responses to a variety of anti-viral agents [17,18]. The 3D/TGP-HuS-E/2 cells have the advantage of being a small-scale 3D cultured cells, which are cultured in 12-well plates at a density of 1×10^5/well, that allow the study of both viral and cellular events. In the current study, it demonstrated a 2 log increase in susceptibility to natural HCV infection and replication when compared to conventional 2D culture systems. Thus it offers an important advantage in the study of natural HCV infection and replication, and the response of natural HCV to anti-HCV drugs.

As the ability of HuS-E/2 cells to support infection and replication of natural HCV was greatly altered by the culture conditions, it is likely that the culture system described in our study will provide important information in regards to the cellular factors that support the HCV life cycle. The microarray study showed that the expression of some genes related to the PPARα signaling pathway were upregulated in the 3D cultured HuS-E/2 cells. Using both PPARα signaling agonists and antagonists, PPARα signaling was shown to affect infection and proliferation of natural HCV. PPARα is a ligand-activated transcription factor that is primarily expressed in tissues with high lipid metabolism including the liver, where it functions as one of three major nuclear receptors and is essential for its normal function [19]. Similar to a part of our data, a negative effect on HCV replication was previously observed in the replicon-bearing cells treated with siRNA for PPARα, with only 50% reduction of HCV-RNA [20]. In this study, even a large dose of PPARα agonist enhanced natural HCV replication in the 2D-HuS-E/2 cells for three times, despite the 2 logs enhancement of HCV proliferation in 3D/TGP culture. This implies that additional factors activated in 3D/TGP-HuS-E/2 cells may be required for the efficient HCV proliferation. Further analysis of the microarray data may provide us with further information on factors that may prove useful in the development of anti-HCV drugs.

In conclusion, the novel *in vitro* culture system combining TGP and immortalized hepatocytes described in this study demonstrated efficient support of natural HCV infection and replication. This system may be used in future virological studies to define new anti-HCV strategies. It may also prove useful for the specific design of effective individual therapy according to patient-specific strains.

Acknowledgments

This work was supported by Grants-in-Aid from the Ministry of Health, Labor and Welfare of Japan; and for scientific research from Ministry of Education, Sports, Culture, and Technology of Japan.

References

[1] Z. Younossi, J. Kallman, J. Kincaid, The effects of HCV infection and management on health-related quality of life, Hepatology 45 (2007) 806–816.

[2] M.W. Fried, M.L. Shiffman, K.R. Reddy, C. Smith, G. Marinos, F.L. Goncales Jr., D. Haussinger, M. Diago, G. Carosi, D. Dhumeaux, A. Craxi, A. Lin, J. Hoffman, J. Yu, Peginterferon alfa-2a plus ribavirin for chronic hepatitis C virus infection, N. Engl. J. Med. 347 (2002) 975–982.
[3] K. Murakami, K. Ishii, Y. Ishihara, S. Yoshizaki, K. Tanaka, Y. Gotoh, H. Aizaki, M. Kohara, H. Yoshioka, Y. Mori, N. Manabe, I. Shoji, T. Sata, R. Bartenschlager, Y. Matsuura, T. Miyamura, T. Suzuki, Production of infectious hepatitis C virus particles in three-dimensional cultures of the cell line carrying the genome-length dicistronic viral RNA of genotype 1b, Virology 351 (2006) 381–392.
[4] G. Andrei, Three-dimensional culture models for human viral diseases and antiviral drug development, Antiviral Res. 71 (2006) 96–107.
[5] H.H. Aly, K. Watashi, M. Hijikata, H. Kaneko, Y. Takada, H. Egawa, S. Uemoto, K. Shimotohno, Serum-derived hepatitis C virus infectivity in interferon regulatory factor-7-suppressed human primary hepatocytes, J. Hepatol. 46 (2007) 26–36.
[6] K. Goto, K. Watashi, T. Murata, T. Hishiki, M. Hijikata, K. Shimotohno, Evaluation of the anti-hepatitis C virus effects of cyclophilin inhibitors, cyclosporin A, and NIM811, Biochem. Biophys. Res. Commun. 343 (2006) 879–884.
[7] T. Murata, M. Hijikata, K. Shimotohno, Enhancement of internal ribosome entry site-mediated translation and replication of hepatitis C virus by PD98059, Virology 340 (2005) 105–115.
[8] M.A. El-Farrash, H.H. Aly, K. Watashi, M. Hijikata, H. Egawa, K. Shimotohno, In vitro infection of immortalized primary hepatocytes by HCV genotype 4a and inhibition of virus replication by cyclosporin, Microbiol. Immunol. 51 (2007) 127–133.
[9] J. Samulin, I. Berget, S. Lien, H. Sundvold, Differential gene expression of fatty acid binding proteins during porcine adipogenesis, Comp. Biochem. Physiol. B: Biochem. Mol. Biol. 151 (2008) 147–152.
[10] S. Hummasti, B.A. Laffitte, M.A. Watson, C. Galardi, L.C. Chao, L. Ramamurthy, J.T. Moore, P. Tontonoz, Liver X receptors are regulators of adipocyte gene expression but not differentiation: identification of apoD as a direct target, J. Lipid Res. 45 (2004) 616–625.
[11] C.G. Walker, M.J. Holness, G.F. Gibbons, M.C. Sugden, Fasting-induced increases in aquaporin 7 and adipose triglyceride lipase mRNA expression in adipose tissue are attenuated by peroxisome proliferator-activated receptor alpha deficiency, Int. J. Obes. (Lond.) 31 (2007) 1165–1171.
[12] D.G. Jump, D. Botolin, Y. Wang, J. Xu, B. Christian, O. Demeure, Fatty acid regulation of hepatic gene transcription, J. Nutr. 135 (2005) 2503–2506.
[13] D.W. Crabb, S. Liangpunsakul, Alcohol and lipid metabolism, J. Gastroenterol. Hepatol. 21 (Suppl. 3) (2006) S56–S60.
[14] D. Panigrahy, A. Kaipainen, S. Huang, C.E. Butterfield, C.M. Barnes, M. Fannon, A.M. Laforme, D.M. Chaponis, J. Folkman, M.W. Kieran, PPARalpha agonist fenofibrate suppresses tumor growth through direct and indirect angiogenesis inhibition, Proc. Natl. Acad. Sci. USA 105 (2008) 985–990.
[15] V.S. Deshpande, J.P. Kehrer, Mechanisms of *N*-acetylcysteine-driven enhancement of MK886-induced apoptosis, Cell Biol. Toxicol. 22 (2006) 303–311.
[16] K.J. Blight, A.A. Kolykhalov, C.M. Rice, Efficient initiation of HCV RNA replication in cell culture, Science 290 (2000) 1972–1974.
[17] R.C. Dickson, Clinical manifestations of hepatitis C, Clin. Liver Dis. 1 (1997) 569–585.
[18] E.J. Heathcote, Antiviral therapy: chronic hepatitis C, J. Viral Hepat. 14 (Suppl. 1) (2007) 82–88.
[19] C.N. Palmer, M.H. Hsu, K.J. Griffin, J.L. Raucy, E.F. Johnson, Peroxisome proliferator activated receptor-alpha expression in human liver, Mol. Pharmacol. 53 (1998) 14–22.
[20] B. Rakic, S.M. Sagan, M. Noestheden, S. Belanger, X. Nan, C.L. Evans, X.S. Xie, J.P. Pezacki, Peroxisome proliferator-activated receptor alpha antagonism inhibits hepatitis C virus replication, Chem. Biol. 13 (2006) 23–30.

JOURNAL OF VIROLOGY, Nov. 2008, p. 10375–10385 Vol. 82, No. 21
0022-538X/08/$08.00+0 doi:10.1128/JVI.00395-08

Hepatitis C Virus Infection Induces Apoptosis through a Bax-Triggered, Mitochondrion-Mediated, Caspase 3-Dependent Pathway▽

Lin Deng,[1] Tetsuya Adachi,[1] Kikumi Kitayama,[1] Yasuaki Bungyoku,[1] Sohei Kitazawa,[2] Satoshi Ishido,[3] Ikuo Shoji,[1] and Hak Hotta[1]*

Divisions of Microbiology[1] and Molecular Pathology,[2] Kobe University Graduate School of Medicine, 7-5-1 Kusunoki-cho, Chuo-ku, Kobe 650-0017, and Laboratory for Infectious Immunity, Riken Research Center for Allergy and Immunology, 1-7-22 Suehiro-cho, Tsurumi-ku, Yokohama, Kanagawa 230-0045,[3] Japan

Received 23 February 2008/Accepted 20 August 2008

We previously reported that cells harboring the hepatitis C virus (HCV) RNA replicon as well as those expressing HCV NS3/4A exhibited increased sensitivity to suboptimal doses of apoptotic stimuli to undergo mitochondrion-mediated apoptosis (Y. Nomura-Takigawa, et al., J. Gen. Virol. 87:1935–1945, 2006). Little is known, however, about whether or not HCV infection induces apoptosis of the virus-infected cells. In this study, by using the chimeric J6/JFH1 strain of HCV genotype 2a, we demonstrated that HCV infection induced cell death in Huh7.5 cells. The cell death was associated with activation of caspase 3, nuclear translocation of activated caspase 3, and cleavage of DNA repair enzyme poly(ADP-ribose) polymerase, which is known to be an important substrate for activated caspase 3. These results suggest that HCV-induced cell death is, in fact, apoptosis. Moreover, HCV infection activated Bax, a proapoptotic member of the Bcl-2 family, as revealed by its conformational change and its increased accumulation on mitochondrial membranes. Concomitantly, HCV infection induced disruption of mitochondrial transmembrane potential, followed by mitochondrial swelling and release of cytochrome *c* from mitochondria. HCV infection also caused oxidative stress via increased production of mitochondrial superoxide. On the other hand, HCV infection did not mediate increased expression of glucose-regulated protein 78 (GRP78) or GRP94, which are known as endoplasmic reticulum (ER) stress-induced proteins; this result suggests that ER stress is not primarily involved in HCV-induced apoptosis in our experimental system. Taken together, our present results suggest that HCV infection induces apoptosis of the host cell through a Bax-triggered, mitochondrion-mediated, caspase 3-dependent pathway(s).

Hepatitis C virus (HCV) often establishes persistent infection to cause chronic hepatitis, liver cirrhosis, and hepatocellular carcinoma, which is a significant health problem around the world (56). Although the exact mechanisms of HCV pathogenesis, such as viral persistence, liver cell injury, and carcinogenesis, are not fully understood yet, an accumulating body of evidence suggests that apoptosis of hepatocytes is significantly involved in the pathogenesis of HCV (1, 2, 9). It is widely accepted that apoptosis of virus-infected cells is an important strategy of the host to protect itself against viral infections. Apoptotic cell death can be mediated either by the host immune responses through the function of virus-specific cytotoxic T lymphocytes and/or by viral proteins themselves that trigger an apoptotic pathway(s) of the host cell.

Apoptotic pathways can be classified into two groups: the mitochondrial death (intrinsic) pathway and the extrinsic cell death pathway initiated by the tumor necrosis factor (TNF) family members (31, 63). Mitochondrion-mediated apoptosis is initiated by a variety of apoptosis-inducing signals that cause the imbalance of the major apoptosis regulator, the proteins of the Bcl-2 family, such as Bcl-2, Bax, and Bid. For example, the proapoptotic protein Bax accumulates on mitochondria after being activated and triggers an increase in the permeability of the outer mitochondrial membrane. Consequently, the mitochondria release cytochrome *c* and other key molecules that facilitate apoptosome formation to activate caspase 9. This, in turn, activates downstream death programs, such as caspase 3 and poly(ADP-ribose) polymerase (PARP). The mitochondria also release apoptosis-inducing factor and endonuclease G to facilitate caspase-independent apoptosis. On the other hand, the extrinsic cell death pathway involves the activation of caspase 8 through binding to the adaptor protein Fas-associated protein with death domain (FADD), which in turn activates caspase 3 to facilitate cell death.

There have been many studies regarding the HCV protein(s) that is directly involved in apoptosis, identifying the protein as either proapoptotic or antiapoptotic, and some data are inconsistent. For example, core (5, 13, 36, 73), E1 (15, 16), E2 (12), NS3 (48), NS4A (43), and NS5A and NS5B (57) have been reported to induce apoptosis. On the other hand, there are reports showing that core (40, 49, 51), E2 (35), NS2 (21), NS3 (58), and NS5A (33, 67) function as antiapoptotic proteins. However, whether the virus as a whole is proapoptotic or antiapoptotic needs to be studied in the context of virus replication, which is believed to be much more dynamic than mere expression of a viral protein(s).

We previously reported that replication of an HCV RNA replicon rendered the host cell prone to undergoing mitochondrion-mediated apoptosis upon suboptimal doses of apoptosis-inducing stimuli (43). Recently, an efficient virus infection system using a particular clone of HCV genotype 2a and a highly permissive human hepatocellular carcinoma-derived cell line

* Corresponding author. Mailing address: Division of Microbiology, Kobe University Graduate School of Medicine, 7-5-1 Kusunoki-cho, Chuo-ku, Kobe 650-0017, Japan. Phone: 81-78-382-5500. Fax: 81-78-382-5519. E-mail: hotta@kobe-u.ac.jp.

▽ Published ahead of print on 3 September 2008.

has been developed (37, 38, 66, 71). In this study, by using the virus infection system, we examined the possible effect of HCV infection on the fate of the host cell. We report here that HCV infection induces apoptosis via the mitochondrion-mediated pathway, as demonstrated by the increased accumulation of the proapoptotic protein Bax on the mitochondria, decreased mitochondrial transmembrane potential, and mitochondrial swelling, which result in the release of cytochrome *c* from the mitochondria and the activation of caspase 3.

MATERIALS AND METHODS

Cells. The Huh7.5 cell line (6), a highly HCV-susceptible subclone of Huh7 cells, was a kind gift from C. M. Rice, Center for the Study of Hepatitis C, The Rockefeller University. The cells were propagated in Dulbecco's modified Eagle medium supplemented with 10% heat-inactivated fetal bovine serum and 0.1 mM nonessential amino acids.

Virus. The virus stock used in this study was prepared as described below. The pFL-J6/JFH1 plasmid, encoding the entire viral genome of a chimeric strain of HCV genotype 2a, J6/JFH1 (37), was kindly provided by C. M. Rice. The plasmid was linearized by XbaI digestion and in vitro transcribed by using T7 RiboMAX (Promega, Madison, WI) to generate the full-length viral genomic RNA. The in vitro-transcribed RNA (10 μg) was transfected into Huh7.5 cells by means of electroporation (975 μF, 270 V) using Gene Pulser (Bio-Rad, Hercules, CA). The cells were then cultured in complete medium, and the supernatant was propagated as an original virus (J6/JFH1-passage 1 [J6/JFH1-P1]). Since the infectious titer of the original virus was not high enough for infection of all the cells in the culture at once, an adapted strain of the virus was obtained by passaging the virus-infected cells 47 times. The adapted virus (J6/JFH1-P47), which is a pool of adapted mutants, possesses 10 amino acid mutations (K78E, T396A, T416A, N534H, A712V, Y852H, W879R, F2281L, M2876L, and T2925A) and a single nucleotide mutation in the 5′-untranslated region (U146A) and produces a much higher titer of infectivity in Huh7.5 cell cultures than the original J6/JFH1-P1 (our unpublished data). Virus infection was performed at a multiplicity of infection of 2.0. Culture supernatants of uninfected cells served as a control (mock preparation).

Virus infectivity was measured by indirect immunofluorescence analysis, as described below, and expressed as cell-infecting units/ml.

Cell viability/proliferation assay. Huh7.5 cells were seeded in 96-well plates at a density of 1.0×10^4 cells/well and cultured overnight. The cells were then infected with the virus or the mock preparation, and, at different time points, cell viability/proliferation was determined by the WST-1 assay (Roche, Mannheim, Germany), as described previously (43).

Detection of apoptosis. The degree of apoptosis was measured by using a Cell Death Detection ELISA^{Plus} kit (Roche), which is based on the determination of cytoplasmic histone-associated DNA fragments, according to the manufacturer's protocol. In brief, cells cultured in a 96-well plate were centrifuged at $200 \times g$ for 10 min at 4°C to remove the supernatant. After the cells were lysed with lysis buffer, the plate was centrifuged at $200 \times g$ for 10 min to separate the cytoplasmic and nuclear fractions. Twenty microliters of supernatant was placed in each well of a streptavidin-coated 96-well plate. Subsequently, a mixture of biotin-labeled anti-histone antibody and peroxidase-labeled anti-DNA antibody was added and wells were incubated for 2 h at room temperature. After wells were washed three times to remove the unbound components, peroxidase activities were determined photometrically with 2,2′-azino-diethyl-benzthiazolin sulfonate as a substrate and measured by using a microplate reader (Bio-Rad).

Caspase enzymatic activities. Activities of caspase 3, 8, and 9 were measured by using Caspase-Glo 3/7, 8, and 9 assays (Promega), respectively, according to the manufacturer's instructions. In brief, a proluminescence caspase 3/7, 8, or 9 substrate, which consists of aminoluciferin (substrate for luciferase) and the tetrapeptide sequence DEVD, LETD, or LEHD (cleavage site for caspase 3/7, 8, or 9, respectively), was added to cultured cells in each well of a 96-well plate, and the plate was incubated for 30 min at room temperature. In the presence of caspase 3/7, 8, or 9, aminoluciferin was liberated from the proluminescence substance and utilized as a substrate for the luciferase reaction. The resultant luminescence in relative light units was measured by using a Luminescencer-JNR AB-2100 (Atto, Tokyo, Japan).

Cell fractionation. Cells were fractionated by using a mitochondrial isolation kit (Pierce, Rockford, IL), according to the manufacturer's instructions. Briefly, 2×10^7 cells were harvested and suspended in reagent A containing a protease inhibitor cocktail (Roche). The cell suspension was mixed with buffer B, vortexed for 5 min, and then mixed with reagent C. The nuclei and unbroken cells were removed by centrifugation at $700 \times g$ for 10 min at 4°C, and the supernatant was used as cell lysate. The cell lysate was further centrifuged at $3,000 \times g$ for 15 min at 4°C. The pellet obtained, which was considered the mitochondrial fraction, was washed once with reagent C and dissolved in a lysis buffer containing 10 mM Tris-HCl (pH 7.5), 150 mM NaCl, 1 mM EDTA, 1% NP-40, and a protease inhibitor cocktail. The remaining supernatant was further centrifuged at $100,000 \times g$ for 30 min at 4°C, and the resultant supernatant was collected as a cytosolic fraction.

To verify successful mitochondrial fractionation, the cytosolic and mitochondrial fractions were analyzed by immunoblotting, as described below, using antibody against Tim23, a mitochondrion-specific protein.

Analysis of the mitochondrial transmembrane potential. The mitochondrial transmembrane potential was measured by flow cytometry using the cationic lipophilic green fluorochrome rhodamine 123 (Rho123; Sigma, St. Louis, MO), as described previously (43). Briefly, cells (7×10^5) were harvested, washed twice with phosphate-buffered saline (PBS), and incubated with Rho123 (0.5 μg/ml) at 37°C for 25 min. The cells were then washed twice with PBS, and Rho123 intensity was analyzed by a flow cytometer (Becton Dickinson, San Jose, CA). A total of 10,000 events were collected per sample. Mean fluorescence intensities were measured by calculating the geometric mean for each histogram peak.

Detection of morphological changes of the mitochondria. Mitochondrial morphology was analyzed by two different methods. (i) For fluorescence microscopy, Huh7.5 cells seeded on glass coverslips in a 24-well plate were incubated for 30 min at 37°C with 100 nM MitoTracker (Molecular Probes, Eugene, OR). After being washed twice with PBS, the cells were fixed with 3.7% paraformaldehyde and observed under a confocal laser scanning microscope (Carl Zeiss, Oberkochen, Germany). When needed, the fixed cells were subjected to indirect immunofluorescence to confirm HCV infection, as described below. (ii) Electron microscopy was performed as described previously (23, 43). In brief, cells were fixed with 4% paraformaldehyde and 0.2% glutaraldehyde for 30 min at room temperature. After being washed with PBS, the cells were collected, dehydrated in a series of 70%, 80%, and 90% ethanol, embedded in LR White resin (London Resin, Berkshire, United Kingdom), and kept at −20°C for 2 days to facilitate resin polymerization. After ultrathin sectioning, samples were etched in 3% H_2O_2 for 5 min at room temperature and washed with PBS. Sections were stained with uranyl acetate and lead citrate and observed under a transmission electron microscope (JEM 1299EX; JOEL, Tokyo, Japan).

Detection of mitochondrial superoxide. Cells seeded on glass coverslips in a 24-well plate were incubated with 5 μM MitoSOX Red (Molecular Probes) at 37°C for 10 min. After being washed with warm Hanks' balanced salt solution with calcium and magnesium (Invitrogen, Carlsbad, CA), the cells were fixed with 3.7% paraformaldehyde and observed under a confocal laser scanning microscope (Carl Zeiss). When needed, the fixed cells were subjected to indirect immunofluorescence to confirm HCV infection, as described below.

Indirect immunofluorescence. Cells seeded on glass coverslips in a 24-well plate at a density of 6×10^4 cells/well were infected with HCV or left uninfected. At different time points after virus infection, the cells were fixed with 3.7% paraformaldehyde in PBS for 15 min at room temperature and permeabilized in 0.1% Triton X-100 in PBS for 15 min at room temperature. After being washed with PBS twice, cells were consecutively stained with primary and secondary antibodies. Primary antibodies used were anti-active caspase 3 rabbit polyclonal antibody (Promega) and an HCV-infected patient's serum. Secondary antibodies used were Cy3-conjugated donkey anti-rabbit immunoglobulin G (IgG; Chemicon, Temecula, CA), Alexa Fluor 594-conjugated goat anti-human IgG (Molecular Probes), and fluorescein isothiocyanate (FITC)-conjugated goat anti-human IgG (MBL, Nagoya, Japan). The cells were washed with PBS, counterstained with Hoechst 33342 solution (Molecular Probes) at room temperature for 10 min, mounted on glass slides, and observed under a confocal laser scanning microscope (Carl Zeiss). The specificity of this immunostaining was confirmed by using mouse monoclonal antibody against HCV core protein (C7-50; Abcam, Tokyo, Japan).

To analyze the possible localization of the activated Bax on mitochondrial membranes, cells were incubated with MitoTracker and subjected to immunofluorescence analysis using rabbit polyclonal antibody against activated Bax (NT antibody; Upstate, Lake Placid, NY). This antibody is directed toward N-terminal residues 1 to 21 of Bax in an N-terminal conformation-dependent manner and specifically recognizes the active form of Bax, in which this segment is exposed in response to apoptotic stimuli (64).

Immunoblotting. Cells were lysed in a buffer containing 10 mM Tris-HCl (pH 7.5), 150 mM NaCl, 1 mM EDTA, 1% NP-40, and a protease inhibitor cocktail (Roche). After two freeze-thaw cycles, cell debris was removed by

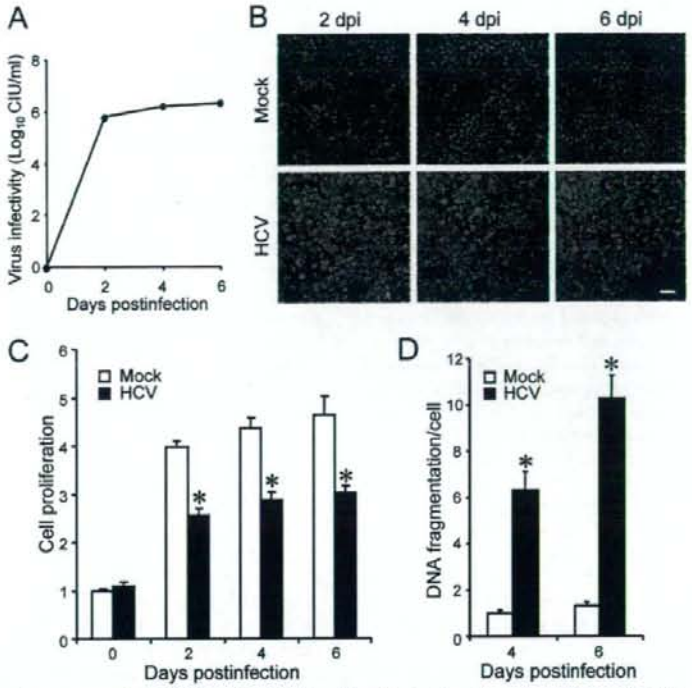

FIG. 1. HCV infection induces apoptosis in Huh7.5 cells. (A) Virus infectivity in the culture supernatants of HCV-infected cells. (B) Detection of HCV antigens in the cells. Huh7.5 cells mock inoculated or inoculated with HCV were subjected to indirect immunofluorescence analysis to detect HCV antigens (red staining) using an HCV-infected patient's serum and Alexa Fluor 594-conjugated goat anti-human IgG at 2, 4, and 6 days postinfection (dpi). Nuclei were counterstained with Hoechst 33342 (blue staining). Scale bar, 50 μm. (C) Cell viability/proliferation was measured for HCV-infected cultures and the mock-inoculated controls. Proliferation of the control cells at day 0 postinfection was arbitrarily expressed as 1.0. Data represent means ± standard deviations (SD) of three independent experiments. *, $P < 0.01$, compared with the control. (D) DNA fragmentation was measured as an index of apoptotic cell death for HCV-infected cultures and the mock-inoculated controls. DNA fragmentation of the control cells at 4 days postinfection was arbitrarily expressed as 1.0. Data represent means ± SD of three independent experiments. *, $P < 0.01$, compared with the control.

centrifugation. Protein quantification was carried out using a bicinchoninic acid protein assay kit (Pierce). Equal amounts of soluble proteins (4 to 20 μg) were subjected to sodium dodecyl sulfate-polyacrylamide gel electrophoresis and transferred onto a polyvinylidene difluoride membrane (Millipore, Bedford, MA), which was then incubated with the respective primary antibody. The primary antibodies used were mouse monoclonal antibodies against cytochrome *c* (A-8; Santa Cruz Biotechnology, Santa Cruz, CA), HCV NS3 (Chemicon), Tim23, Bax and Bcl-2 (BD Biosciences Pharmingen, San Diego, CA); rabbit polyclonal antibodies against Bak (Upstate), caspase 3, and PARP (Cell Signaling Technology, Danvers, MA); and goat polyclonal antibodies against glucose-regulated protein 78 (GRP78) and GRP94 (Santa Cruz Biotechnology). Horseradish peroxidase-conjugated goat anti-mouse IgG (MBL), goat anti-rabbit IgG (Bio-Rad), and donkey anti-goat IgG (Santa Cruz Biotechnology) were used as secondary antibodies. In some experiments, a commercial kit that facilitates the antigen-antibody reaction (Can Get Signal; Toyobo, Osaka, Japan) was used to obtain stronger signals. The respective protein bands were visualized by means of an enhanced chemiluminescence (GE Healthcare, Buckinghamshire, United Kingdom), and the intensity of each band was quantified by using NIH Image J. Protein loading was normalized by probing with goat antibody against actin (Santa Cruz Biotechnology) as a primary antibody.

Statistical analysis. The two-tailed Student *t* test was applied to evaluate the statistical significance of differences measured from the data sets. A *P* value of <0.05 was considered statistically significant.

RESULTS

HCV infection induces caspase 3-dependent apoptosis in Huh7.5 cells. We first examined virus growth in Huh7.5 cells. HCV grew efficiently in the culture, and virus titers in the supernatant reached a plateau level at 2 days postinfection (Fig. 1A). Immunofluorescence analysis revealed that >95% of the cells were infected with HCV on the same day (Fig. 1B). To examine the possible impact of HCV infection on the cells, we measured the cell viability/proliferation at 0, 2, 4, and 6 days postinfection. As shown in Fig. 1C, the proliferation of HCV-infected cells was significantly slower than that of the mock-infected control. Similar results were obtained when the parental Huh7 cells were used for HCV infection (data not shown). The observed delay in cell proliferation was associated with an increase in cell death, seen as cell rounding and floating in the culture (data not shown) and in cellular DNA fragmentation (Fig. 1D). As DNA fragmentation is a hallmark of apoptosis, our data suggest that HCV infection induces apoptosis in Huh7.5 cells.

The J6/JFH1-P47 strain of HCV used in this study possesses adaptive mutations compared to the original strain (J6/JFH1-P1). Therefore, we compared the impacts of the two strains on cell viability/proliferation and DNA fragmentation. While both strains caused inhibition of cell proliferation and an increase in DNA fragmentation, J6/JFH1-P47 appeared to exert a stronger cytopathic effect than J6/JFH-P1 (data not shown).

To further verify that HCV infection induces apoptotic cell death, we analyzed caspase 3 activities in HCV-infected Huh7.5 cells and the mock-infected control. As shown in Fig. 2A, caspase 3 activities in HCV-infected cells increased to levels that were 2.2, 6.0, and 12 times higher than that in the control cells at 2, 4, and 6 days postinfection, respectively. We also examined HCV-induced caspase 3 activation by immunoblot analysis. Activation of caspase 3 requires proteolytic processing of its inactive proenzyme into the active 17-kDa and 12-kDa subunit proteins. The anti-caspase 3 antibody used in this analysis recognizes 35-kDa procaspase 3 and the 17-kDa subunit protein. At 6 days postinfection, activated caspase 3 was detected in HCV-infected cells but not in the mock-infected control (Fig. 2B, second row from the top). Analysis of the death substrate PARP, which is a key substrate for active caspase 3 (61), also demonstrated that the uncleaved PARP (116 kDa) was proteolytically cleaved to generate the 89-kDa fragment in HCV-infected cells but not in the mock-infected control (Fig. 2B, third row). Cleavage of PARP facilitates cellular disassembly and serves as a marker of cells undergoing apoptosis (44).

In order to further confirm these observations, indirect immunofluorescence staining was performed by using an anti-active caspase 3 antibody that specifically recognizes the newly exposed C terminus of the 17-kDa fragment of caspase 3 but not the inactive precursor form. As shown in Fig. 2C, the activated form of caspase 3 was clearly observed in HCV-infected cells but not in the mock-infected control at 6 days postinfection. The activation of caspase 3 was observed also at 4 days postinfection (data not shown). We found that caspase 3 activation was detectable in 12% and 21% of HCV antigen-positive cells at 4 and 6 days postinfection, respectively, whereas it was detectable only minimally in mock-infected cells at the same time points (Fig. 2D). These results strongly suggest that HCV-induced cell death is caused by caspase 3-dependent apoptosis. We also observed nuclear translocation of active caspase 3 in HCV-infected cells (Fig. 2E). This result is consistent with previous reports (28, 70) that activated caspase 3 is located not only in the cytoplasm but also in the nuclei of apoptotic cells. Concomitantly, nuclear condensation and shrinkage were clearly observed in the caspase 3-activated cells. As the activation and nuclear translocation of caspase 3 occur before the appearance of the nuclear change, not all caspase 3-activated cells exhibited the typical nuclear changes. Taken together, these results indicate that HCV-induced apoptosis is associated with activation and nuclear translocation of caspase 3.

HCV infection induces the activation of the proapoptotic protein Bax. The proteins of the Bcl-2 family are known to directly regulate mitochondrial membrane permeability and induction of apoptosis (63). Therefore, we examined the expression levels of proapoptotic proteins, such as Bax and Bak, and antiapoptotic protein Bcl-2 in HCV-infected Huh7.5 cells and the mock-infected control. The result showed that expression levels of Bak or Bcl-2 did not differ significantly between HCV-infected cells and the control. Interestingly, however, Bax accumulated on the mitochondria in HCV-infected cells to a larger extent than in the mock-infected control (Fig. 3A), with the average amount of mitochondrion-associated Bax in HCV-infected cells being 2.7 times larger than that in the control cells at 6 days postinfection (Fig. 3B).

In response to apoptotic stimuli, Bax undergoes a conformational change to expose its N and C termini, which facilitates translocation of the protein to the mitochondrial outer membrane (32). Thus, the conformational change of Bax represents a key step for its activation and subsequent apoptosis. We therefore investigated the possible conformational change of Bax in HCV-infected cells by using a conformation-specific NT antibody that specifically recognizes the Bax protein with an exposed N terminus. As shown in Fig. 3C, Bax staining with the conformation-specific NT antibody was readily detectable in HCV-infected cells at 6 days postinfection whereas there was no detectable staining with the same antibody in the mock-infected control. Moreover, the activated Bax was shown to be colocalized with MitoTracker, a marker for mitochondria, in HCV-infected cells. The conformational change of Bax was observed in 10% and 15% of HCV-infected cells at 4 and 6 days postinfection, respectively (Fig. 3D). This result was consistent with what was observed for caspase 3 activation in HCV-infected cells (Fig. 2D). Taken together, these results suggest that HCV infection triggers conformational change and mitochondrial accumulation of Bax, which lead to the activation of the mitochondrial apoptotic pathway.

HCV infection induces the disruption of the mitochondrial transmembrane potential, release of cytochrome *c* from mitochondria, and activation of caspase 9. The accumulation of Bax on the mitochondria is known to decrease the mitochondrial transmembrane potential and increase its permeability, which result in the release of cytochrome *c* and other key molecules from the mitochondria to the cytoplasm to activate caspase 9. Therefore, we examined the possible effect of HCV infection on mitochondrial transmembrane potential in Huh7.5 cells. Disruption of the mitochondrial transmembrane potential was indicated by decreased Rho123 retention and, hence, decreased fluorescence. As shown in Fig. 4, HCV-infected cells showed ~50% and ~70% reductions in Rho123 fluorescence intensity compared with the mock-infected control at 4 and 6 days postinfection, respectively.

Recent studies have indicated that loss of mitochondrial membrane potential leads to mitochondrial swelling, which is often associated with cell injury (27, 50). Also, we and other investigators have reported that HCV NS4A (43), core (53), and p7 (22) target mitochondria. We therefore analyzed the effect of HCV infection on mitochondrial morphology. Confocal fluorescence microscopic analysis using MitoTracker revealed that mitochondria began to undergo morphological changes at 4 days postinfection and that approximately 40% of HCV-infected cells exhibited mitochondrial swelling and/or aggregation compared with the mock-infected control at 6 days postinfection (Fig. 5A and B). It should also be noted that mitochondrial swelling and/or aggregation was seen in a region different from the "membranous web," where the HCV replication complexes accumulate to show stronger expression of

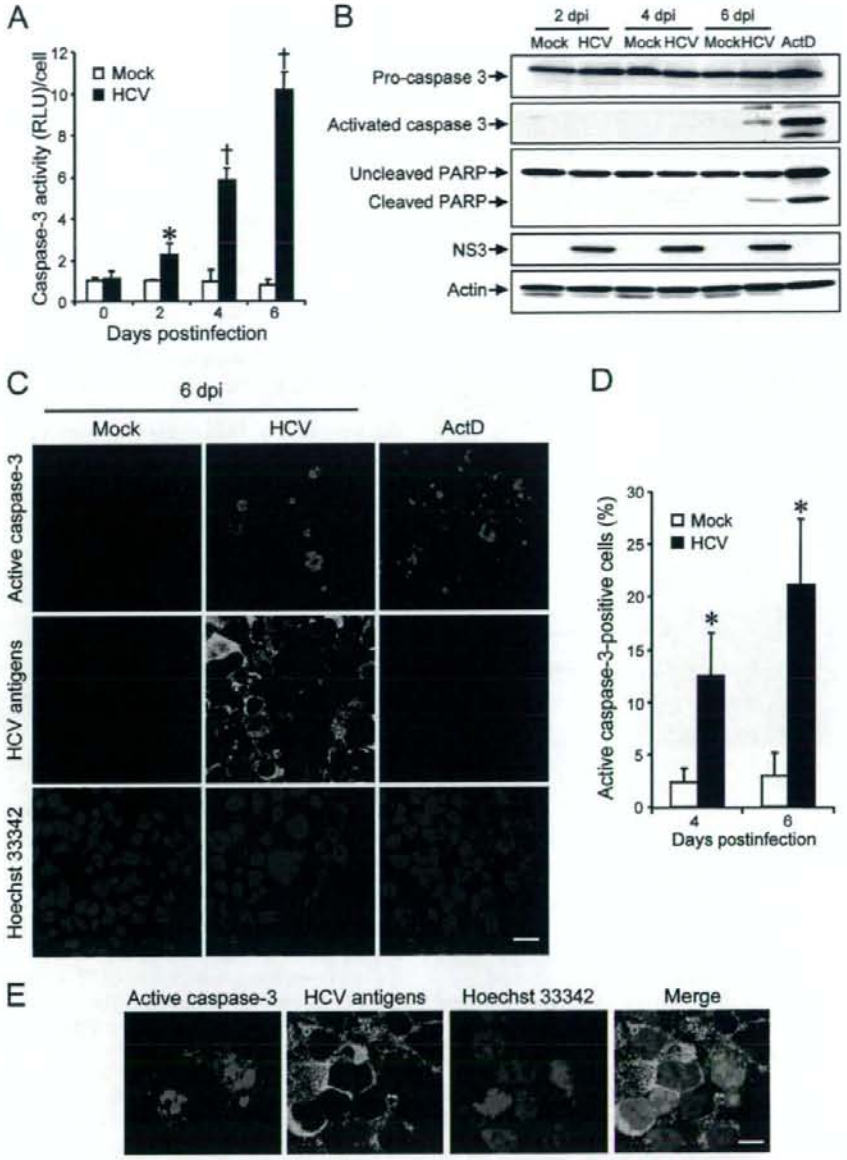

FIG. 2. HCV infection activates caspase 3 in Huh7.5 cells. (A) Caspase 3 activities in cells infected with HCV and mock-infected controls. The caspase 3 activity of the control cells at day 0 postinfection was arbitrarily expressed as 1.0. *, $P < 0.05$; †, $P < 0.01$ (compared with the control). Data represent means ± standard deviations (SD) of three independent experiments. (B) Immunoblot analysis to detect the activated form of caspase 3 (~17 kDa) and cleavage product of PARP (~85 kDa) in HCV-infected cells and the mock-infected control at 2, 4, and 6 days postinfection (dpi). Huh7.5 cells treated with actinomycin D (ActD; 50 ng/ml) for 30 h served as a positive control. Amounts of actin were measured as an internal control to verify an equal amount of sample loading. (C) Huh7.5 cells infected with HCV or mock infected were subjected to indirect immunofluorescence analysis at 6 dpi. Cells treated with ActD (50 ng/ml) for 30 h served as a positive control. After fixation and permeabilization, the cells were incubated with anti-active caspase 3 rabbit polyclonal antibody followed by Cy3-labeled donkey anti-rabbit IgG (top) and with an HCV-infected patient's serum followed by FITC-labeled goat anti-human IgG (middle). The cells were then stained with Hoechst 33342 for the nuclei (bottom). Scale bar, 20 μm. (D) Quantification of active caspase 3-expressing cells. The percentages of cells expressing active caspase 3 were determined for HCV-infected cultures and mock-infected controls. Data represent means ± SD of three independent experiments. *, $P < 0.05$, compared with the control. (E) Nuclear translocation of active caspase 3 in HCV-infected cells. Subcellular localization of active caspase 3 in HCV-infected cells was examined by indirect immunofluorescence analysis at 6 days postinfection as described in the legend for panel C. Scale bar, 5 μm.

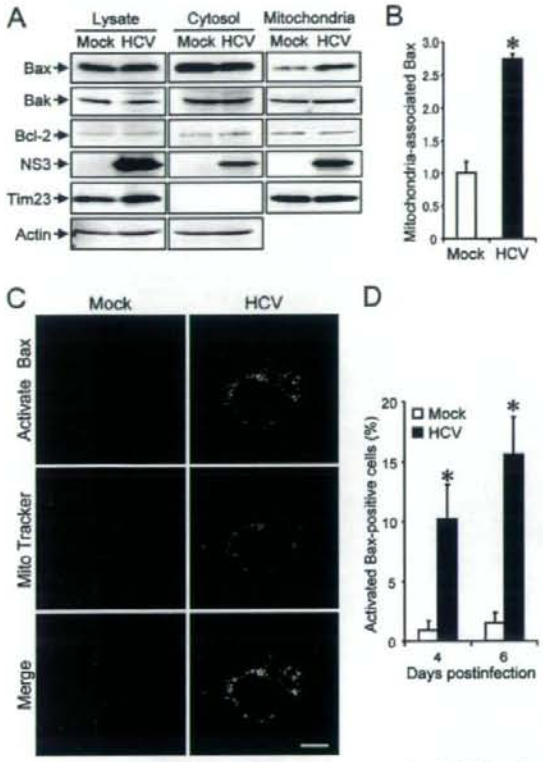

FIG. 3. HCV infection induces Bax activation in Huh7.5 cells. (A) Accumulation of Bax on the mitochondria in HCV-infected Huh7.5 cells. Cytosolic and mitochondrial fractions as well as whole-cell lysates were prepared from HCV-infected cells and the mock-infected control at 6 days postinfection and analyzed by immunoblotting using antibodies against Bax, Bak, Bcl-2, NS3, Tim23, and actin. Amounts of Tim23, a mitochondrion-specific protein, were measured to verify equal amounts of mitochondrial fractions. Amounts of actin were measured to verify equal amounts of whole-cell lysates and cytosolic fractions. (B) The intensities of the bands of mitochondrion-associated Bax in HCV-infected cells and the mock-infected control were quantified. The intensity of the mock-infected control was arbitrarily expressed as 1.0. Data represent means ± standard deviations (SD) of three independent experiments. *, $P < 0.01$, compared with the control. (C) Conformational change of Bax in HCV-infected cells. Huh7.5 cells infected with HCV and the mock-infected control were subjected to indirect immunofluorescence analysis at 6 days postinfection. After incubation with MitoTracker (middle row), the cells were incubated with an antibody specific for the N terminus of Bax (NT antibody), followed by Alexa Fluor 488-labeled goat anti-rabbit IgG (top row). Merged images are shown on the bottom. Scale bar, 10 μm. (D) Quantification of activated Bax-positive cells. The percentages of cells expressing activated Bax were determined for HCV-infected cultures and the mock-infected control. Data represent means ± SD of three independent experiments. *, $P < 0.01$, compared with the control.

HCV antigens. This observation implies the possibility that an indirect effect(s) of HCV infection, in addition to a direct effect of an HCV protein, as observed for NS3/4A (43), is involved in mitochondrial swelling and/or aggregation.

Electron microscopic analysis also demonstrated swelling and structural alterations of mitochondria in HCV-infected cells, whereas mitochondria remained intact in the mock-infected control (Fig. 5C). This result suggests a detrimental effect of HCV infection on the volume homeostasis and morphology of mitochondria and is consistent with previous observations that liver tissues from HCV-infected patients showed morphological changes in mitochondria (3).

Mitochondrial swelling and the morphological change of mitochondrial cristae are associated with cytochrome *c* release (27, 54). We then examined the effect of HCV infection on cytochrome *c* release in Huh7.5 cells. The result clearly demonstrated cytochrome *c* release from the mitochondria to the cytoplasm in HCV-infected cells but not in the mock-infected control (Fig. 6A). The release of cytochrome *c* from mitochondria is known to induce activation of caspase 9 (31). We then analyzed caspase 9 activities in the cells. As shown in Fig. 6B, caspase 9 activities in HCV-infected cells increased to levels that were ca. five times higher than that in the control cells at 4 and 6 days postinfection.

HCV infection induces a marginal degree of caspase 8 activation. In addition to the mitochondrial death (intrinsic) pathway described above, the extrinsic cell death pathway, which is initiated by the TNF family members and mediated by activated caspase 8 (31, 62), is also the focus of attention in the study of apoptosis. Therefore, we examined caspase 8 activities in HCV-infected cells and the mock-infected control. As shown in Fig. 6C, caspase 8 activities in HCV-infected cells increased to a level that was ca. two times higher than that in the control cells at 4 and 6 days postinfection. This increase was much smaller than that observed for caspase 9 activation (Fig. 6B).

HCV infection induces increased production of mitochondrial reactive oxygen species (ROS). The production of ROS, such as superoxide, by mitochondria is the major cause of cellular oxidative stress (8), and a possible link between ROS production and Bax activation has been reported (18, 42). Therefore, we next examined the mitochondrial ROS production in HCV- and mock-infected cells by using MitoSOX, a fluorescent probe specific for superoxide that selectively accumulates in the mitochondrial compartment. As shown in Fig. 7A and B, approximately 25% of HCV-infected cells displayed a much higher signal than did the mock-infected control. This result suggests that oxidative stress is induced by HCV infection.

HCV infection does not induce ER stress. It is well known that HCV nonstructural proteins form the replication complex on the endoplasmic reticulum (ER) membrane (4, 19, 39, 46). It was recently reported that HCV infection (55) as well as the transfection of the full-length HCV replicon (17) and the expression of the entire HCV polyprotein (14) induced an ER stress response. Therefore, we tested whether HCV infection in our system induces ER stress. We adopted increased expression of GRP78 and GRP94 as indicators of ER stress (34) and, as a positive control, used tunicamycin to induce ER stress (20, 25). As had been expected, the expression levels of GRP78 and GRP94 were markedly increased in Huh7.5 cells when cells were treated with tunicamycin for 48 h (Fig. 8, right). On the other hand, HCV infection did not alter expression levels of GRP78 or GRP94 at 2, 4, or 6 days postinfection compared

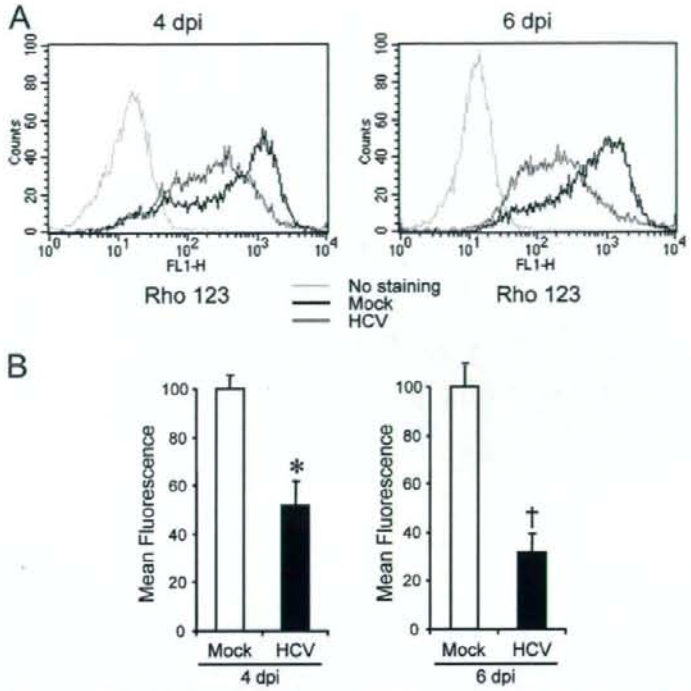

FIG. 4. HCV infection induces disruption of the mitochondrial transmembrane potential in Huh7.5 cells. (A) Huh7.5 cells infected with HCV and the mock-infected control were stained with Rho123 and subjected to flow cytometric analysis to measure the mitochondrial transmembrane potential at 4 and 6 days postinfection (dpi). The red and black lines represent Rho123 staining of HCV-infected cells and the mock-infected control, respectively. The green profiles represent staining of the cells with PBS alone. (B) Mean fluorescence intensities of HCV-infected cells and the mock-infected control at 4 and 6 dpi. Data represent means ± standard deviations (SD) of three independent experiments. *, $P < 0.05$; †, $P < 0.01$ (compared with the control).

with those for the mock-infected control (Fig. 8). This result suggests that ER stress, if there is any, is marginal and does not play an important role in HCV-induced apoptosis in Huh7.5 cells.

DISCUSSION

The mitochondrion is an important organelle for cell survival and death and plays a crucial role in regulating apoptosis. An increasing body of evidence suggests that apoptosis occurs in the livers of HCV-infected patients (1, 2, 9) and that HCV-associated apoptosis involves, at least partly, a mitochondrion-mediated pathway (2). In those clinical settings, however, it is not clear whether apoptosis is mediated by host immune responses through the activity of cytotoxic T lymphocytes or whether it is mediated directly by HCV replication and/or protein expression itself. In experimental settings, ectopic expression of HCV core (13, 36), E2 (12), and NS4A (43) has been shown to induce mitochondrion-mediated apoptosis in cultured cells. However, these observations need to be verified in the context of virus replication. The recent development of an efficient HCV infection system in cell culture (37, 66, 71) has allowed us to investigate whether HCV replication directly causes apoptosis. In the present study, we have demonstrated that HCV infection induces Bax-triggered, mitochondrion-mediated, caspase 3-dependent apoptosis, as evidenced by increased accumulation of Bax on mitochondria and its conformational change (Fig. 3), decreased mitochondrial transmembrane potential (Fig. 4), and mitochondrial swelling (Fig. 5), which lead to the release of cytochrome *c* from the mitochondria (Fig. 6A) and subsequent activation of caspase 9 and caspase 3 (Fig. 6B and 2, respectively).

We also observed increased production of mitochondrial superoxide in HCV-infected cells (Fig. 7). This result is consistent with previous observations that expression of the entire HCV polyprotein (47) or HCV replication (60) enhanced production of ROS, including superoxide, through deregulation of mitochondrial calcium homeostasis. ROS, which are produced through the mitochondrial respiratory chain (8), were reported to trigger conformational change, dimerization, and mitochondrial translocation of Bax (18, 42). It is likely, therefore, that activation of Bax in HCV-infected cells is mediated, at least partly, through increased production of ROS in the mitochondria. Kim et al. (29) reported that ROS is a potent activator of c-Jun N-terminal protein kinase, which can phosphorylate Bax, leading to its activation and mitochondrial translocation. In

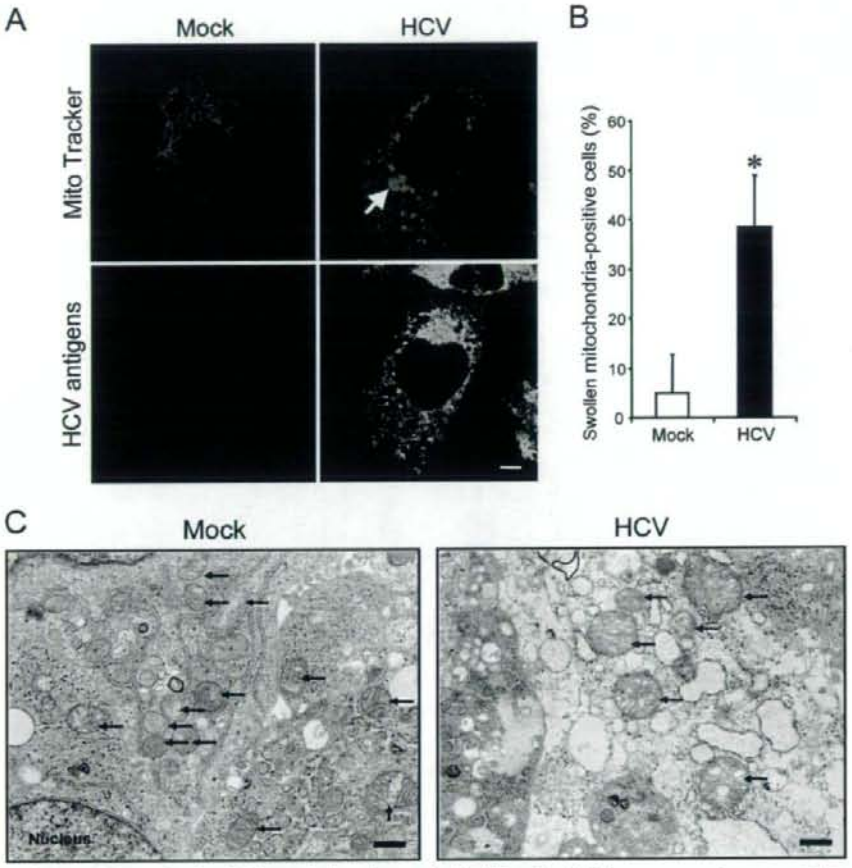

FIG. 5. HCV infection induces mitochondrial morphology changes in Huh7.5 cells. (A) Fluorescence microscopy analysis. Mitochondrial morphologies of HCV-infected cells and the mock-infected control at 6 days postinfection were examined by confocal microscopy. The cells were directly incubated with MitoTracker (upper row) and then stained for HCV antigens by using an HCV-infected patient's serum, followed by FITC-labeled goat anti-human IgG (bottom row). Scale bar, 5 μm. (B) Quantification of swollen mitochondrion-positive cells. The percentages of cells exhibiting swollen and/or aggregated mitochondria were determined for HCV-infected cultures and the mock-infected control. Data represent means ± standard deviations of three independent experiments. *, $P < 0.01$, compared with the control. (C) Electron microscopic analysis. Mitochondrial morphologies of HCV-infected cells and the mock-infected control at 6 days postinfection were examined by electron microscopy. Arrows indicate mitochondria. Scale bar, 1 μm.

this connection, HCV core protein has been shown to play a role in generating mitochondrial ROS (30). It was also reported that HCV core protein bound to the 14-3-3□protein to dissociate Bax from the Bax/14-3-3□complex, thereby promoting the Bax translocation to the mitochondria (36).

In addition to the caspase 9 activation that is mediated through the mitochondrial death (intrinsic) pathway, caspase 8 activation was seen in HCV-infected cells, though to a lesser extent (Fig. 6B and C). Caspase 8 is a key component of the extrinsic death pathway initiated by the TNF family members (31, 62). This pathway involves death receptors, such as Fas, TNF receptor, and TNF-related apoptosis-inducing ligand (TRAIL) receptors, which transduce signals to induce apoptosis upon binding to their respective ligands (52). In HCV-infected patients, the Fas-mediated signal pathway is involved in apoptosis of virus-infected hepatocytes (24). It was also reported that HCV (JFH1 strain) infection induced apoptosis through a TRAIL-mediated pathway in LH86 cells (72). On the other hand, a caspase 9-mediated activation of caspase 8, which is considered a cross talk between the intrinsic and the extrinsic death pathways, in certain cell systems was also reported (10, 11, 65). Whether the observed caspase 8 activation in HCV-infected cells was mediated through the extrinsic death pathway initiated by a cytokine(s) produced in the culture or whether it was mediated through the cross talk between the intrinsic and the extrinsic death pathways awaits further investigation. In this connection, activated caspase 8 is known to cleave the proapoptotic protein Bid to generate the Bid